Maximum Power Exploitation for Grid-connected PV System under Fast-varying Solar Irradiation Levels with Modified Salp Swarm Algorithm

Mingxuan Mao[1, 2, *], Li Zhang[4], Han Huang[3], Benjamin Chong[4], Lin Zhou[2]

[1]Postdoctoral Station of Electrical Engineering Chongqing University, Chongqing 400044, China

[2]School of Electrical Engineering, Chongqing University, Chongqing 400044, China

[3]Energy Safety Research Institute, Swansea University, Swansea SA1 8EN, Wales, United Kingdom

[4]School of Electronic and Electrical Engineering, University of Leeds, Leeds LS2 9JT, United Kingdom

Abstract: With the rapid development of photovoltaic (PV) power generation technology, PV generation system has been appliedintoplanes, cars, boats and trains. Solar irradiation levels will change rapidly in these PV systems. Fast-varying solar irradiation can invalidate the traditional configurations of PV system and maximum power point tracking (MPPT) control strategy, which will reduce the energy conversion efficiency. In order to extract maximum power exploitation, this paper proposes a novel maximum power exploitation configuration combined with the proposed control schemefor grid-connected PV system under fast-varying solar irradiation levels. In the proposed configuration, each PV panel cascades a step-up boost converter, hence allowing independent control corresponding to the irradiation levels, which generates multiple-levels of dc-voltage and may be converted to ac via anactive neutral point clamped (ANPC) inverter. Meanwhile, a modified salp swarm algorithm with dynamic *w* factor (DWSSA) based MPPT method is proposed for each boost converter units, which can effectively accelerate convergence velocity and stability of iteration to make the searching process rapidly adapting to different fast-varying solar irradiation levels. In order to express the dynamic variation of the PV system, the mathematical model of the proposed configuration is established. Moreover, the performance of the proposed DWSSA algorithm is investigated by the stability analysis based Lyapunov theory and convergence analysis on 23 benchmark functions and CEC 2005 benchmark functions.Finally, the constructed simulation test platform is implemented and the results demonstrate that the configuration can exploit the variable converter ratios, and the proposed DWSSA method has faster tracking speed and higher energy extractionefficiency compared with the previous MPPT methods in most cases, especially, the power extraction percentage of 97.89% and the tracking time of 0.761s under the most severe uneven solar irradiation levels.

Keywords: Solar energy exploitation;multilevel boostconverters;MPPT; Modified salp swarm algorithm;Fast-varying solar irradiation

NOTATION

v_{on}	dc-dc converter terminalvoltage	x_e	equilibrium state
V_{pvn}	PV source voltage	$S(\delta)$	initial state domain
D_n	duty ratio	$S(\varepsilon)$	state solution domain
C_{on}	PV-converter capacitor	$x_{\max}$	equilibrium point
I_{pvn}	PV source current	$f(x_{\max})$	the optimal value
i_{link}	DC-linkcurrent	$f(x_{\max2})$	the sub-optimal value
R	equivalent resistive load	$D_{\max}$	the optimal region
$\vec{v}_{out}$	ANPC terminal voltage	ub_j	the upper bound
M_a	amplitude modulation index	lb_j	the lower bound
i_G	grid current	L	the maximum iterations
v_G	grid voltage	l	the current iteration
R_f	filter resistance	v_0	the initial speed
L_f	filter inductor	w^*	dynamic factor
V_{DC}	sum of individual PV-boost converter voltage	ϕ	random value within the interval (0,1)
j	number of dimensions	$f(x)$	objective function
x^1_j	the first salp position	f	Lipschitz in solution x
F_j	the food source position	δ	the radii of one domain

1 Introduction

The exhaustible nature of fossil energy source and the increasing environmental preservation requirementsmake it more than ever necessary the development of clean and sustainable power generation sources. Among all the cleaner renewable energy resources, the sustainability, abundancy, ubiquity and inexhaustibility of solar energy contribute to it becoming the most essential resource in recent years (Villalvaet al., 2009). Solar energy has experienced improved efficiency and price decline in the past two decades (Ashouri-Zadehet al., 2018). However, photovoltaic (PV) power generation as an important form of solar energy utilizationstill faces efficiency limits. PV panel plays a vital role in converting solar energy to electrical energy in a PV power generationsystem. Hence, the capability to extract the maximum power from PV panels independently on the panel temperature, solar irradiation, shading conditions and PV cell ageing plays an essential role.Especially,solar irradiance level has an very important impact on the maximum power exploitation, when the PV panel is installed on the moving carriers, such as planes, cars, boats and trains, thus continuously subjected to fast-varyingsolar irradiation levels (Rizzoet al., 2018).

For PV power generationsystemunder fast-varying solar irradiation levels, the mismatch concern among serialPV panels is one of the main causes of losses in the power extraction from the systems. They are originated from the interaction betweenserialPV panels with different solar irradiation levelsunder variableoperating conditions.Specifically, PV panelsare exposed to different values of irradiance and the PV panel exposed to lower irradiance will absorb the energysupplied by the PV panel exposed to higher irradiance, leading to highly localized power dissipation and converting this power into heat (Martinet al., 2018).Meanwhile, the fast-varying solar irradiationcan make the former MPPT algorithms may fail to achieve the MPP. Therefore, by investigating the aspects of the panel performance evaluation and optimization for electricity production under fast-varying solar irradiation levels, the configurations optimal for PV panel system and the control schemes for the maximum power generation need to be designed to guarantee maximum power exploitation of the PV power generation systemunder fast-varying solar irradiation levels.

Conventional PV power systems configurations are that several PV modules are connected in series and a central DC-DCconverter or DC-AC inverter is used as the power interface withthe load or grid (Luo et al., 2016).Typical topologies for the micro-converter include the buck (Urtasunet al., 2015), boost (Urtasunet al., 2013), buck-boost (Chen et al., 2014), modified buck-boost converter (Wu et al., 2016), SEPIC (Chianget al., 2009), and zeta converter (Kumar and Singh, 2014). Walker and Sernia in (Walker and Sernia, 2004) have examined four different types of dc-dc converters, though they did not include grid connection.The system proposed by Abdalla et al. (2016) extended this configuration by connecting several PV-buck dc-dc converter modules in a chain and controlling each module independently to obtain MPPT according to their respective irradiation level. The works in (Prabaharan and Palanisamy, 2016) uses boost dc-dc converters for each PV module, but also it does not include grid connection part. More recent work included direct connection to ac grid, the approach used is to give each PV module its own dc-ac inverter, commonly the full H-bridge, hence forming the module integrated PV ac-converter unit. Although the above typical topologies work for the current common PV system, aimed at the moving carriers, these topologies obviously cannot meet its requirements of the moving carriers PV systemunder fast-varying solar irradiation levels, and needs to be improved.

Considering the nonlinearity of the PV moduleswith the irradiation and temperature variation, MPPTalgorithms are necessarily used in order toensure the PV modules operated in optimal states under any environmentalconditions and mismatch insolation conditions (Batarseh and Za'Ter, 2018). Specifically, the conventional well-known MPPT methods, such asthe design of boost converter based on maximum power point resistance (Ayop and Tan, 2018), the tangent error MPPT algorithm based on perturb and observe method (P&O) (Penget al., 2018),the novel temperature controller and incremental conductance MPPT algorithm(INC) (Shahidet al., 2018),fuzzy logic controller-based MPPT(FLC) (Khan and Mathew, 2018), etc.,get stuck in local MPPs or incur considerable computationalcost.Alternative approaches use evolutionary algorithms such as PSO algorithm (Liet al., 2018), AFSA (Maoet al., 2016), ABC (Soufyaneet al., 2015)，SFLA(Maoet al., 2018)，GWO (Mohantyet al., 2016), FA (Teshomeet al., 2017), and DE(Teyet al., 2018), etc., present good performance of global MPPT under partial shading conditions with no additional circuit configuration, no power output interruption, high tracking accuracy, fast convergence and other advantages.The general description of these common MPPT algorithms is shown Table 1.However, the search performance of most evolutionary algorithms is highly dependent on the parameters of the algorithms, such as inertia coefficient and learning factor in PSO, variation and crossover factor in genetic algorithm and DE, etc.. Improper parameter setting will lead to various problems such as reduced convergence rate or even non-convergence of the algorithms.Salp swarm algorithm (SSA) (Mirjalili et al., 2017) is a simulation of deep ocean salp community behavior of new type of evolutionary algorithm, with its unique group update mechanism, which greatly reduced the possibility of local extremum. SSA outperforms the existing evolutionary algorithms, such asPSO, ABC, SFLA,etc., on the search speed and precision. In particular, SSA has few control parameters, which can effectively avoid the problem that the optimization fails due to the unreasonable parameter setting. In addition, there are few studies on the SSAapplied to MPPT control in the PV system at present.Based on the above analysis, it can be seen that the existing MPPT method will not certainly reach the optimal effect of tracking the MPP in the moving carriers PV system, so the MPPT control method based SSA for the PV system under fast-varying solar irradiation levels can be further studied.

Table 1 The description of some MPPT algorithms

Algorithm	Reference	Description
P&O	(Penget al., 2018)	Based on the mathematical model of optimal voltage, a dynamic perturbation step is calculated by using tangent error method in order to weaken the influence of fast multi-changing solar irradiances.
INC	(Shahidet al., 2018)	A variable step sized incremental conductance (INC)method is combined with the temperature controller to smooth the output power of the PV panel under the changing temperature and irradiance.
FLC	(Khan and Mathew, 2018)	The developed fuzzy logic controller (FLC)-based MPPT method is used to optimize the output of the proposed hybrid system with variable inputs to extract maximum power.
PSO	(Liet al., 2018)	A novel overall distribution algorithm

		integrated with particle swarm optimization (PSO) MPPT algorithm to rapidly search the area near theglobal maximum power points and further improve the accuracy of MPPT.
AFSA	(Maoet al., 2016)	Combining the searching capabilities of PSO and the self-learning ability of adaptive visual and step for artificial fish swarm algorithm (AFSA), modified AFSAtechnique based on the global MPPT is developed.
ABC	(Soufyaneet al., 2015)	A novel artifificial bee colony algorithm based MPPT that gives a simple and a robust scheme is proposed for PV system under dynamic weather conditions.
SFLA	(Maoet al., 2018)	By applying PSO with an extended memory and incorporating the grouping concept from shuffled frog leaping algorithm (SFLA), an advanced searching algorithm is presented for Grid-connected PV System under PSCs.
GWO	(Mohantyet al., 2016)	To overcome the limitations such as lower tracking effificiency, steady-state oscillations, and transients as encountered in P&O and improved PSO techniques, anew MPPT design using grey wolf optimization (GWO)technique for PVsystem under PSCs.
FA	(Teshomeet al., 2017)	A modified firefly algorithm (FA) method that reduce the number of computation operations and the time for converging to global maximum point that the existing FA requires is proposed for PVsystem under PSCs.
DE	(Teyet al., 2018)	An improved global search space differential evolution (DE) algorithm is introduced to improvethe capability of global MPPT within a larger operating region and quicken respond against load variation.

This paper proposes a new configuration for the PV system comprising a chain of module integrated PV step-up boost converter units with the novel MPPT controller and one half-bride ANPC inverter.The use of boost converter for each module offers the benefit of raising the individual PV voltages to higher levels, and importantly, it can realize MPPT according to each module’s respective light levels.

Furthermore, a novel DWSSA based MPPT method is presented which is adopted from the proposedDWSSA, reducing parameter setting to adopt the fast-varying irradiation variations. Applying the proposed DWSSA method to the chained PV-boost converter units plus ANPC configuration, the MPPs for n PV-boost converter units can be initially searched simultaneously and the predicted voltages are applied respectively to control the individual boost converter units. Finally, simulation test platform is constructed for the novel maximum power exploitation configuration with the proposed MPPT method to verify the performance under fast-varying solar irradiation levels.

The rest of the paper is organized as follows: Section 2 presents the methodology, including: reviews the configuration of the proposed grid-connected PVsystem,the mathematical model of the system, the MPPT control strategy for boost converter units and the control strategy for ANPC inverter. Results and discussion are in Section 3, which is made up of the stability and convergence analysis of DWSSAalgorithm and simulation studies of DWSSAfor the proposed grid-connected PVsystem. Section 4concludes this paper.

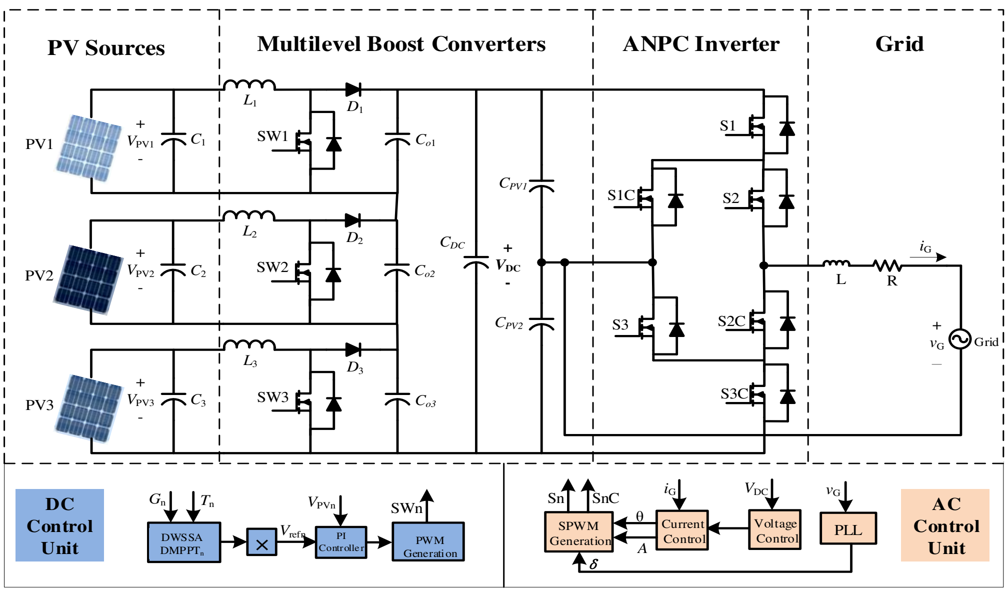

Figure 1 Configuration of the grid-connected PV system

2 Methodology

2.1 Configuration of the proposed grid-connected PVsystem

The configuration of the proposed grid-connected PV system is shown in Figure 1. Each of boost converter units can be installed a DWSSA-MPPT controller to turn on or off its corresponding switch (SWn). The ANPC converter (Floricauet al., 2008) is derived from the 3-level neutral-point clamping converter, with the neutral-point clamping diodes replaced by bidirectional switches.

2.2 Mathematical model of the system

The model expressing the dynamic variation of the above system can be derived as follows. The voltages across each of the dc-dc converter terminals, v_{o1}, v_{o2}, …v_{on}, can be expressed as functions of their respective PV source voltages, V_{pv1}, V_{pv2}, …V_{pvn} and the corresponding switching duty ratios D_1, D_2, …D_n, thus we have

$$v_{on} = \frac{1}{1-D_n} v_{PVn} \tag{1}$$

The currents through capacitors across each PV-converter capacitor C_{o1}, C_{o2}, …C_{on} aredetermined by their respective PV source currents (I_{pv1}, I_{pv2}, …I_{pvn}) and that flowing to theDC-link (i_{link}) and converter duty ratios.

$$\sum i_{C_{on}} = C_{on}\frac{dv_{on}}{dt} = i_{PVn}\cdot(1-D_n) - i_{link} \tag{2}$$

Assuming an equivalent resistive load R is supplied, the current flowing from the DC-link, is given as

$$i_{link} = \frac{v_{o1}+v_{o2}+v_{o3}+\cdots v_{on}}{R} = \frac{v_{pv1}}{R(1-D_1)} + \frac{v_{pv2}}{R(1-D_2)} + \cdots \tag{3}$$

Substitutingi_{link}in eqs. (2) by (3), we have

$$\frac{dv_{on}}{dt} = \frac{1}{C_{on}}\left(i_{PVn}(1-D_n) - \left(\frac{v_{pv1}}{R(1-D_1)} + \frac{v_{pv2}}{R(1-D_2)} + \cdots \frac{v_{pvn}}{R(1-D_n)}\right)\right) \tag{4}$$

For ac part the ANPC terminal voltage $\vec{v}_{out}$ is determined by the amplitude modulation index M_a and the total dc-link voltage which is the sum of individual PV-boost converter voltage as

$$\vec{v}_{out} = M_a V_{DC} = M_a \times \sum_{i=1}^{n} v_{oi} \tag{5}$$

With a simple low-pass R-L filter the current between the PV-converter system and grid is expressed as.

$$L_f\frac{d\vec{i_G}}{dt} = \vec{v}_{out} - \vec{v}_G - R_f\vec{i_G} \tag{6}$$

where i_G and v_G represent the grid current and voltage respectively, R_f and L_f are the filter resistance and inductor. At steady-state and with unity power factor power flow to the grid, ignore losses we should have

$$\vec{v}_G \times i_G = V_{DC} \times i_{link} \tag{7}$$

2.3 MPPT control strategy for boost converter units

Applying the proposed DWSSA MPPT method to the system shown in Figure 1, the searching process is performed on each of the chained PV boost converter units. The initial particles are the a set of randomly selected discrete terminal voltage values from each unit ranging from 0-30V, and there are n of them,

($v_1 \dots v_n$). The fitness function values for each of these particles are evaluated from the PV equivalent circuit model given below.

2.3.1PV model and fitness function

This model used for the shaded PV cell was proposed by J.W. Bishop(Bishop, 2007). The well-known PV equivalent circuit model is shown in Figure 2.Based on the reference (Kermadi and Berkouk, 2017), the fitness functions given as:

$$I_c = I_{sc} - I_o(\exp\left[\frac{q(V_{out} + R_s I_{out})}{AKT_c}\right] - 1) - I_{shunt} \quad (1)$$

$$PVfitness(\mathrm{G,T,I_c}) = I_c \times (V_j - R_s I_c) \quad (2)$$

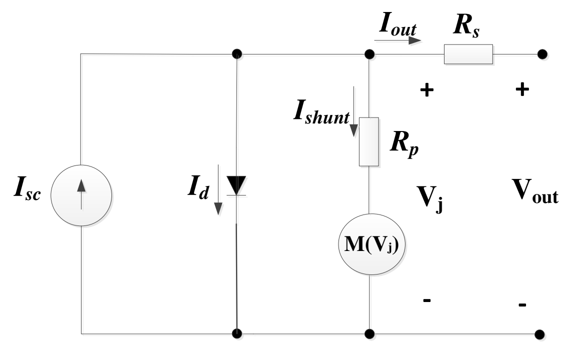

Figure 2PV equivalent circuit model

2.3.2The basic SSAdescription

SSA is proposed by Mirjalili et al. (2017). SSA has few control parameters, which can effectively avoid the problem that the optimization fails due to the unreasonable parameter setting. Specifically, the position of the basic SSA is updated (Mirjaliliet al., 2017):

$$x_j^1 = \begin{cases} F_j + c_1((ub_j - lb_j)c_2 + lb_j), & c_3 \geq 0 \\ F_j - c_1((ub_j - lb_j)c_2 + lb_j), & c_3 < 0 \end{cases} \quad (3)$$

where j is number of dimensions, $x^1{}_j$ and F_j represent respectively the first salp position and the food source position when the number of dimension is j. In addition, ub_j and lb_j is the upper and lower bound respectively when the number of dimension is j, and c_2, c_3 ~U(0, 1). The parameter c_1 is (Mirjaliliet al., 2017):

$$c_1 = 2 \cdot e^{-(\frac{4l}{L})^2} \quad (4)$$

where Land l represent respectively the maximum iterations and the current iteration. The position update formula is (Mirjaliliet al., 2017):

$$x_j^i = \frac{1}{2} a t^2 + v_0 t \tag{5}$$

where v_0 is the initial speed. Considering $v_0 = 0$, the formula will be modified as (Mirjaliliet al., 2017):

$$x_j^i = \frac{1}{2}\left(x_j^i + x_j^{i-1}\right) \tag{6}$$

2.3.4The proposed DWSSA algorithm

In the course of iteration, the followers are influenced by each other. The interactions of followers influence the performance of the population, especially when the algorithm reaches its late iterative stage, the population converges the food source slowly. Therefore, inorder to improve the convergence speed and accuracy, this paper proposes an improved SSA algorithm by introducing a dynamic w factor. Meanwhile, a random value ϕ which is within the interval (0, 1) is added to improve the search ability. Thus, the followers are updated as follows:

$$x_j^i = \frac{1}{2}\left(k * x_j^i + x_j^{i-1}\right) \tag{7}$$

$$k = \phi \cdot w^* \tag{8}$$

$$w^* = w_{\min} + \left(w_{\max} - w_{\min}\right)\left(\frac{L-l}{L}\right) \tag{9}$$

where ϕ is a random value within the interval (0,1), w_{max} =0.9 and w_{min} = 0.2.

2.3.5 DWSSA based MPPTmethod

Applying the DWSSA to the system shown in Figure 1. The flowchart for implementing the DWSSA-MPPT method is shown in Figure 3.

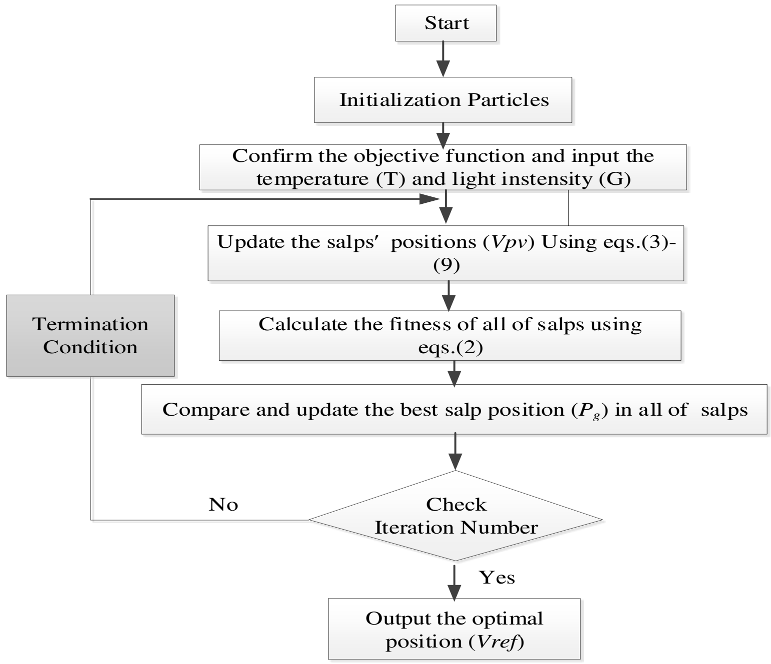

Figure 3 Flowchart of the DWSSA-MPPT method

2.4Control strategy for ANPC inverter

The 3-level ANPC converter is derived from the 3-level NPC converter, with the neutral-point clamping diodes replaced by bidirectional switches as shown in Figure4. The ANPC switches are required to withstand a voltage magnitude of $V_{DC}/2$.The ANPC converter can be controlled by using a double-frequency PWM scheme (DF-PWM) which is known so due to the doubling of the apparent switching frequency at the converter output (Floricauet al., 2008). The DF-PWM scheme results in 4 possible zero-voltage states of the converter, as shown in Table 2.

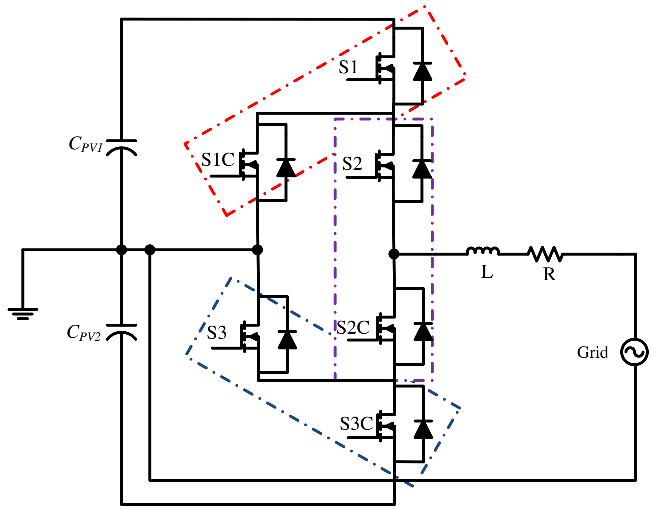

Figure 4 ANPC converter structure

Table 2 Switching sequence of ANPC inverter with DF-PWM

OutputVoltage (V_{NO})	Voltage State	Switch State					
		S1	S1C	S2	S2C	S3	S3C
$-V_{DC}/2$	Negative	0	1	0	1	0	1
0	Zero-Negative (1)	0	0	0	1	1	0
	Zero-Negative (2)	0	1	1	0	0	1
	Zero-Positive (1)	0	1	1	0	0	0
	Zero-Positive (2)	1	0	0	1	1	0
$V_{DC}/2$	Positive	1	0	1	0	1	0

3 Results and discussion

3.1 The stability analysis of DWSSAalgorithm

3.1.1 Stability analysisof DWSSA algorithm based Lyapunov theory

At present, the stability of intelligent algorithms is analyzed and proved by the theoretical knowledge of control systems owing to the lack of mathematical theory. Its methods mainly include Laplace Transform, Lyapunov Stability Theory (Khalil, 2015), Routh Criterion, Z-transform and so on. Becausethe position update formula ofDWSSAalgorithm is too simple to obtain the characteristic equation, this paper uses Lyapunov Stability Theory to analyze the stability of the DWSSA algorithm.

3.1.2 Equilibrium states

If $f(x)$ is objective function of the DWSSA algorithm, then state equation as follow:

$$\dot{x} = f(x,t) \quad (10)$$

where f is continuous in time t and locally Lipschitz in solution$x$. The $\delta$and ε represents the radii of the two domains respectively. For any given ε>0, which corresponds to $\delta(\varepsilon,t_0)>0$, and δ, $\varepsilon \in R$.The solution $x$corresponding any initial state x_0 that satisfying $\|x - x_e\| \le \delta(\varepsilon, t_0)$ satisfies equation (11) at all times.

$$\|x - x_e\| \le \varepsilon \qquad (t \ge t_0) \tag{11}$$

Then the equilibrium state x_e of the system is stable. If $\delta$is independent of t_0, then thex_e is uniformly stable. If all state solutions x starting from the initial state domain $S(\delta)$ do not exceed the state solution domain $S(\varepsilon)$ at all times, then x_e is stable.

Furthermore, $x_{max}$is defined as the equilibrium point under Lyapunov Stability Theory, prove as follows.

According to (10), if$t \to \infty$, $x$will be the best advantage x_{max}. namely:

$$\lim_{t \to \infty} \|x(t : x_0, t_0) - x_e\| = 0 \tag{12}$$

Translate state equation down by x_{max} length, then the new state equation can be obtained:

$$\dot{x} = f(x,t) - f(x_{max}) \tag{13}$$

And then the equilibrium state is satisfied for all of t:

$$\dot{x}_e = f(x_e,t) - f(x_{max}) = 0 \quad (14)$$

Hence, the DWSSA algorithm has an equilibrium point x_{max}, equilibrium state $\dot{x}_e = f(x_{max}, t)$.

3.1.3 Stability analysis based Lyapunov theory

When the DWSSA algorithm performs a global search, the positions of the salps are guided by the a, the β and the δ, and are randomly updated. When the DWSSA algorithm performs the optimal area, the salps will follow the hunting method and will only approach the prey (optimal position x_{max}). Therefore, the global stability can be obtained by analyzing the stability of the optimal region.

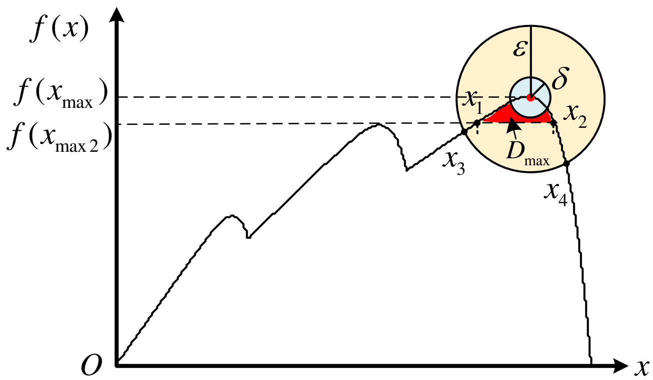

Figure 5 The schematic diagram of the optimal region

A schematic diagram of the optimal region under Lyapunov Stability Theory is shown in Figure5. The $f(x_{max})$ and $f(x_{max2})$ represent the optimal value and the sub-optimal value of the objective function, respectively; D_{max} is the optimal region with a range of $[x_1, x_2]$; x_3 and x_4 are the intersections of the $S(\varepsilon)$ and the $f(x)$. The center of the circle of the $S(\delta)$and the $S(\varepsilon)$ is the global best advantage x_{max}.

The initial state $x(t_0;\ t_{0,}\ x_0)$ is in the D_{max}, that is, the area where the $S(\delta)$ intersects with the objective function $f(x)$ is included by D_{max}. The DWSSA algorithm will only approach the x_{max}, namely:

$$\begin{cases}\delta \le \min(\|x_{\max}-x_1\|,\|x_{\max}-x_2\|) \\ \delta \le \min(f(x_{\max})-f(x_3), f(x_{\max})-f(x_4)) \le \varepsilon\end{cases} \tag{15}$$

For any given $\varepsilon > 0$, there always exists δ that satisfies equation (15), and $\delta, \varepsilon \in R$. It makes the motion starting from any initial state x_0 satisfying any inequality $\|x - x_e\| \le \delta(\varepsilon, t_0)$ satisfy the inequality (16):

$$\|x(t; x_0, t_0) - x_{\max}\| \le \delta \le \varepsilon \tag{16}$$

$$\lim_{t\to\infty}\|x(t : x_0, t_0) - x_e\| = \lim_{t\to\infty}\|x(t : x_0, t_0) - x_{\max}\| = 0 \tag{17}$$

Hence, the solutions of the equations $x(t;x_0,t_0)$ are all in $S(\delta)$, and the radius δ is independent of t_0.

In summary, the equilibrium state x_{max} of the DWSSA algorithm is not only stable under the Lyapunov stability theory, but also the equilibrium state is uniformly asymptotically stable.

3.2 Convergence analysis of DWSSAalgorithm based benchmark functions

3.2.1Convergence analysison 23 benchmark functions

To validate the effectiveness of the proposed DWSSA algorithm, theconvergence analysis based on 23 unimodal, multimodal, and fixed-dimenstion multimodal benchmark functions in Appendix A is implemented, and search space of the representative unimodal, multimodal, and fixed-dimenstion multimodal functions are shown in Figure 6. In addition, it has been compared with other algorithms including PSO and SSA algorithms. To make a fair comparison among PSO (Kennedy and Eberhart, 1995), AFSA(Li, 2002), SSA (Mirjaliliet al., 2017), SSAPSO(Ali et al., 2018), ABC(Karaboga et al., 2007), ALO(Mirjaliliet al., 2015), DA(Mirjaliliet al., 2016), GOA(Saremi et al., 2017), MFO(Mirjaliliet al., 2015), MVO(Mirjaliliet al., 2016), SCA(Mirjaliliet al., 2016), SSA-GWO(Wanet al., 2019) and DWSSA, these algorithms adopt the parameter settings as follows: the population size is 50, and all algorithms run 20 times independently and are stopped when the maximum number of 10000 function evaluations (FEs) is reached in each run. And the results are the Best (the optimal value of the objective function found byeach algorithm), Mean (the mean value of the objective function found byeach algorithm), STD (the standard deviation value of the objective function found byeach algorithm) and Time (the average running time for a run taken byeach algorithm) values of all the runs.

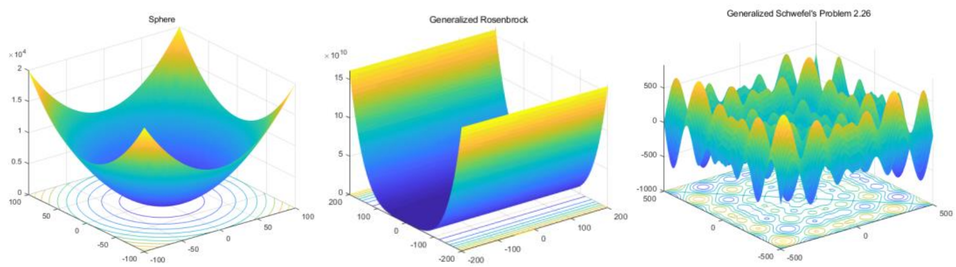

$f_1 f_5 f_8$

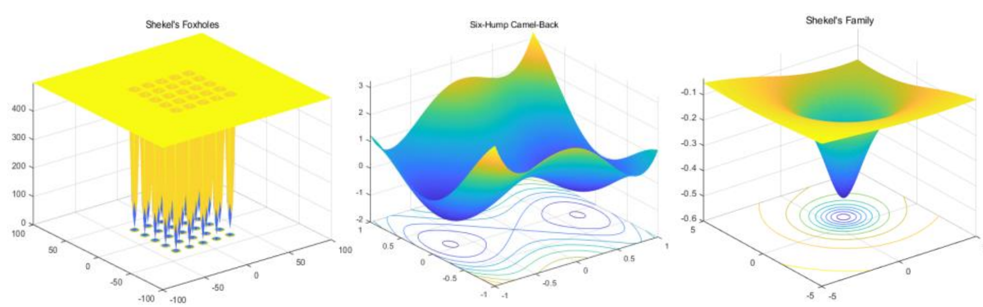

$f_{14} f_{16} f_{22}$

Figure 6 Search space of the representative benchmark test functions

The comparison results obtained by the each algorithm under budgeted FES are given in Appendix B. It can be seen form Appendix B that DWSSA outperforms the other compared algorithms on the most cases. Specially, DWSSA is better than all of the other algorithms on f_1, f_2, f_3, f_4, f_7, f_9, f_{10}, f_{15} and f_{17} cases, respectively, while, PSO, SSAPSO, ALO, DA, GOA, MFO, MVO and SSA-GWO cannot surpass DWSSA on any cases. Moreover, we can see from Figure 6 that DWSSA costs less time than the other SSAs, including SSA, SSAPSO and SSA-GWO, on any cases, while DWSSA does not lose the superiority on the most cases. From Appendix B, some insightful conclusions can be drawn that DWSSA performs more stably than the other algorithms and improves the robustness in performance on the most cases.To graphically highlight the advantages of DWSSA, the convergence curves of 13 algorithms tested on 9 test functions are plotted in Figure 7.Some clear conclusion can be seen from Figure 7 that the convergence speed and precise of DWSSA algorithm are faster and more precise on the most cases. In particular, the convergence precise of the proposed DWSSA is more than 10 orders of magnitude higher than the other algorithms' onf_2, f_4, $f_9$and f_{11} cases, respectively.

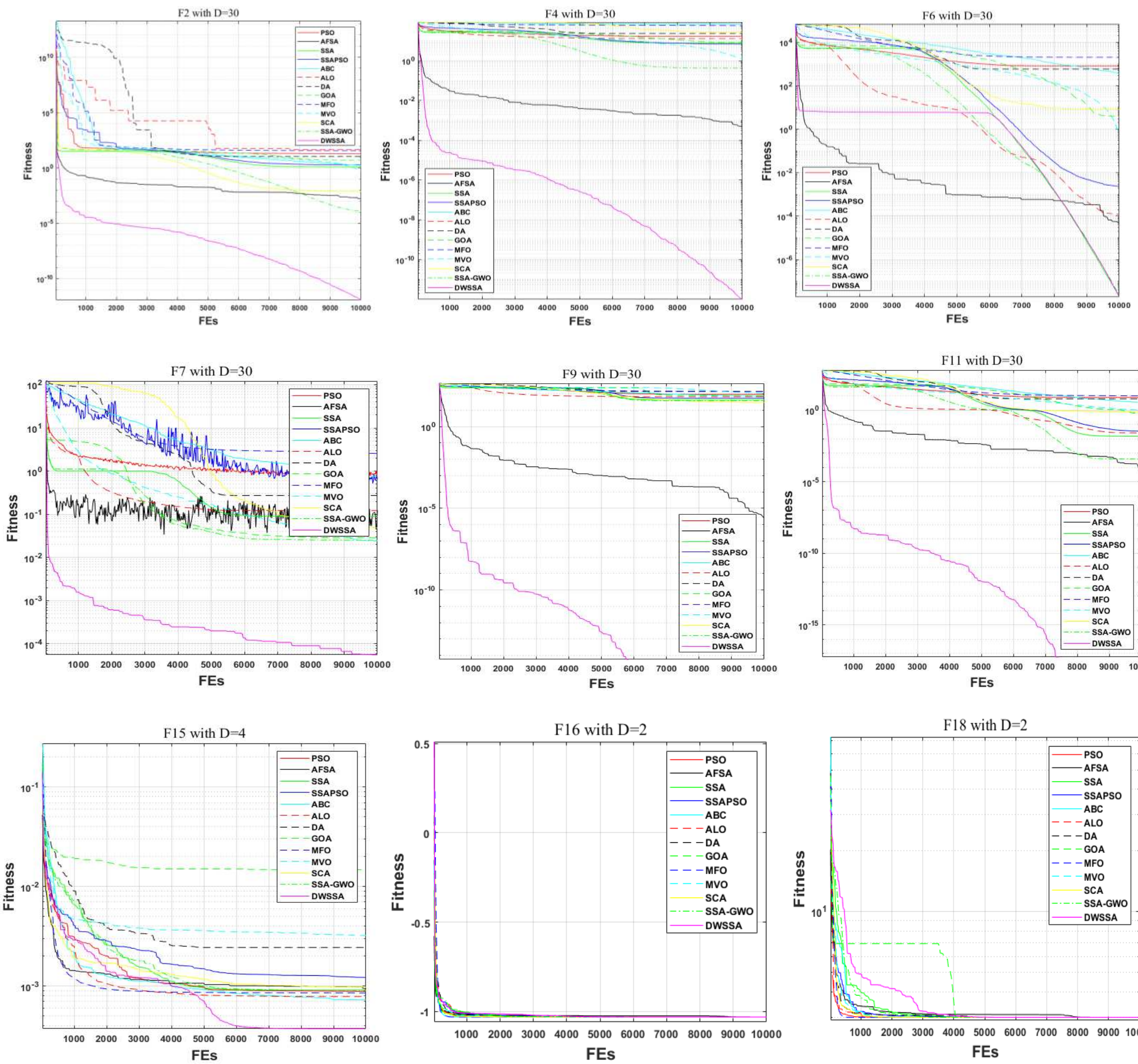

Figure 7 Convergence curves of 13 algorithms

3.2.2Convergence analysis on CEC 2005 benchmark functions

A set of 15 CEC 2005 benchmark functions are chosen to further test the performance of DWSSA. Appendix C shows an introduction to15 functions and Figure 8 gives search space of the representative unimodal, multimodal, multimodal expended, and multimodal hybrid composition CEC 2005 benchmark functions.

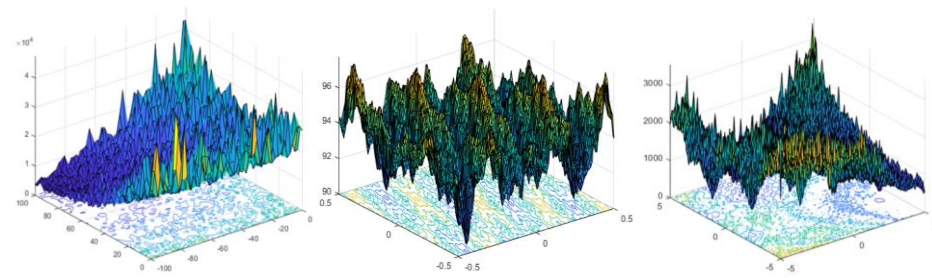

$F_3F_7F_{10}$

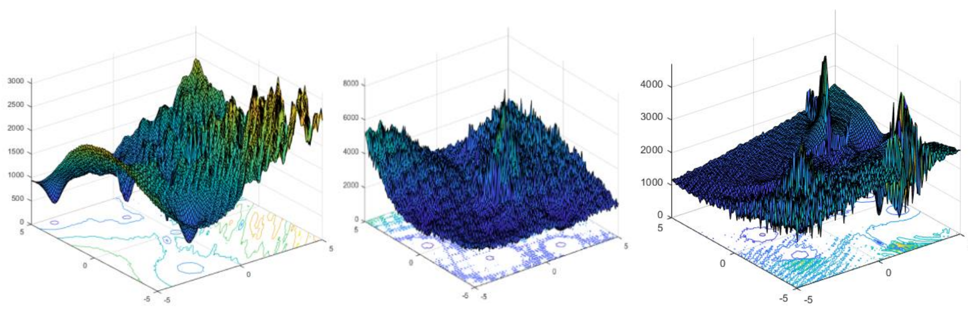

F_{13} F_{14} F_{15}

Figure 8 Search space of the representative benchmark 6 functions

The results of 13 algorithms with the maximum iterations of 500 (5000FEs) are shown in Appendix D. From Appendix D, it can be seen that DWSSA obtains better results than the other competing algorithms on the most cases. Especially, DWSSA greatly outperforms PSO, AFSA, SSA, SSAPSO, ABC, ALO, DA, GOA, MFO, MVO and SCA on F4, F8, F12 and F13. For clarity, Figure 9 gives the convergence curves of 13 algorithms on the representative test functions. Some important conclusion can be observed from Appendix D and Figure 9 that DWSSA outperforms the other compared algorithms in terms of optimization accuracy and stability on the most cases. This is because DWSSA possess the self-adaptive dynamic w factor to balance its exploitation and exploration ability.

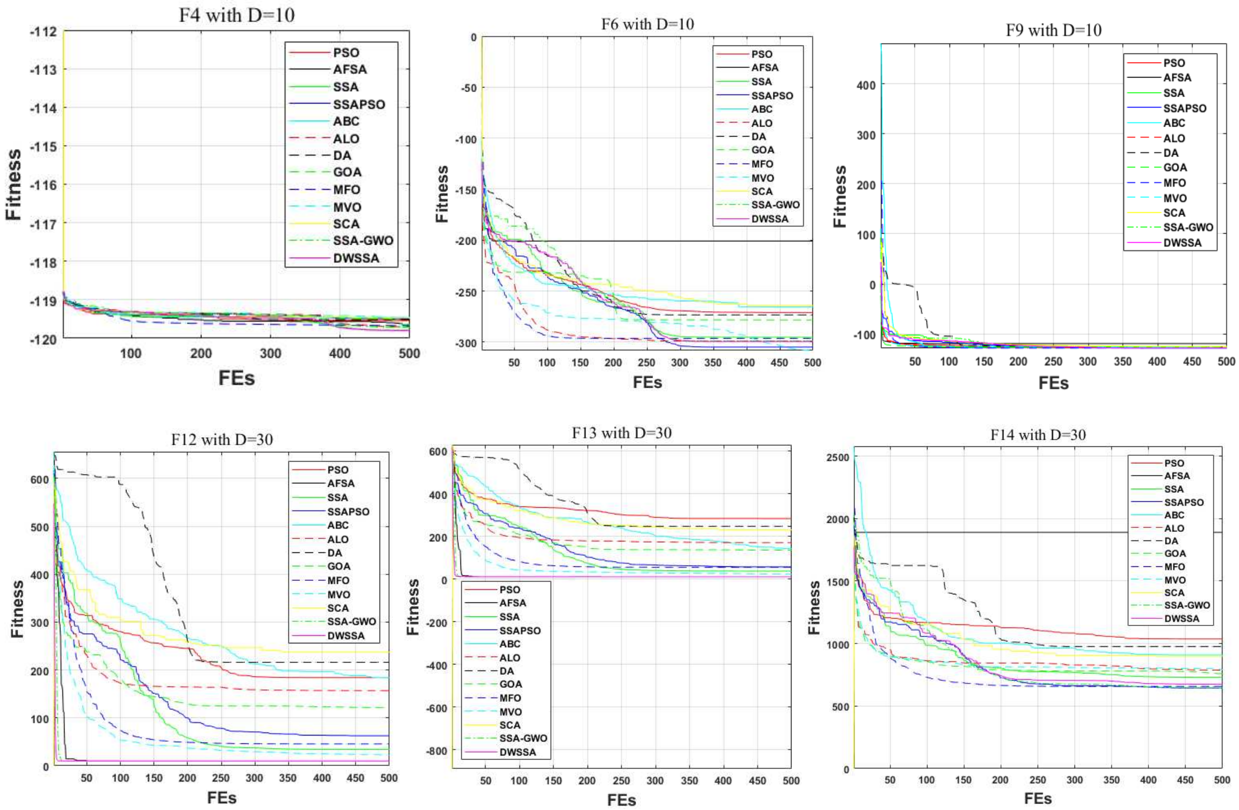

Figure 9 Convergence curves of 13 algorithms on the representative 6 functions

3.3Simulation studies of DWSSAfor the proposed grid-connected PVsystem

3.3.1 The parameter design of the implemented simulation platform

Simulation tests are implemented by using the proposed DWSSA method, traditional P&O method and SSA method, in order to evaluate the proposedconfiguration under the different fast-varying solar irradiation levels. The maximum iteration of SSA, PSO, ABC, AFSA, GWO, SSAGWA, SSAPSO and DWSSA is set to 12, and the number of these algorithms is set to 20. In addition, Table 3 lists the main parameters ofSSA, PSO, ABC, AFSA, GWO, SSAGWA, SSAPSO and DWSSA. The fixed step size of P&O and INC is set as 0.5V. The PV system components parametersare given in Table 4. Moreover,three different irradiance patterns (Case 1-3) and thetwo patternsof low solar irradiation level disturbances (Case a and Case b)listed in Table 5, where G1, G2 and G3 represent the irradiance levels on panels PV1, PV2 and PV3 respectively.Therein, Case a and Case b are used to verify the the convergence precision and stabilityperformance of the proposed algorithm underthe influence ofthe sudden addition of low solar irradiation level disturbances.

Table 3 The main parameters for the two algorithms

Algorithm	Parameter settings
SSA	C_1: Self-adaption
PSO	$C_1 = C_2 = 2$, ω: Self-adaption
ABC	*Limit*=20
AFSA	*Crowd_factor=0.75*
GWO	a: Self-adaption
DWSSA	a and ω: Self-adaption
SSAGWO	a and C_1: Self-adaption
SSAPSO	w and C_{1SSA}: Self-adaption, $C_{1PSO} = C_{2\,PSO} = 2$

Table 4Main component parameters

Symbol	Parameter	Value
P_{mpp}	Maximumpowerofsingle PV module	45W
C_1、C_2、C_3	PV sourceterminalcapacitor	100μF
Co_1、Co_2、Co_3	PV sourceterminalcapacitor	700μF
L_1、L_2、L_3	Inductance	4mH
V_{oc}	Opencircuitvoltage	19.95V
I_{sc}	Short circuit current	3.286A
C_{DC}	DC bus capacitor	1mH
L	Inductance	4.5mH
R	Resistance	0.02Ω
f	AC output frequency	50Hz

Table 5 Irradiance values for three Cases

Case	T = 25°C		
	G_1 (W/m^2)	G_2 (W/m^2)	G_3 (W/m^2)
1	1000	500	800
2	1000	700	1000
a	300	100	200
3	900	700	800
b	200	200	200

3.3.2Simulation results and analysis

The output voltage waveforms of each boost converters using three methods under different cases are shown in Figure 10. Evidently, the unbalance irradiance change among PV units leads to unbalanced voltage distribution for the different boost converter units.It is obviously seen from Figure 10 that the three output voltage waveforms of the converters fluctuates severelywhen the P&O, INC and ABC methodsare employed, while the output voltage of converter is smoother when the DWSSA, SSA, PSO, AFSA, GWO, SSAGWA and SSAPSO methodsare appliedunder the fast-varying solar irradiation levels. In addition, theoutput voltage waveforms of the converterscan be stabilized quicklyunderthe influence ofthe sudden addition of the low solar irradiation level disturbancesexcept the P&O and INC methods in Case a, and the P&O, INC and PSOmethods in Case b.Especially, the output voltage of convertercan be stabilized most quicklyunderthe the sudden addition ofCase a when DWSSAmethod is applied compared to the other 9 algorithms. Therefore, the tracking stability of DWSSA, SSA, PSO, AFSA, GWO, SSAGWA and SSAPSO methods outperform theP&O, INC and ABC methods in all irradiance conditions. Moreover, the tracking accuracy and rapidity of the proposed DWSSA methodhave outstanding performance in Case a and Case b of the low solar irradiation level disturbances.

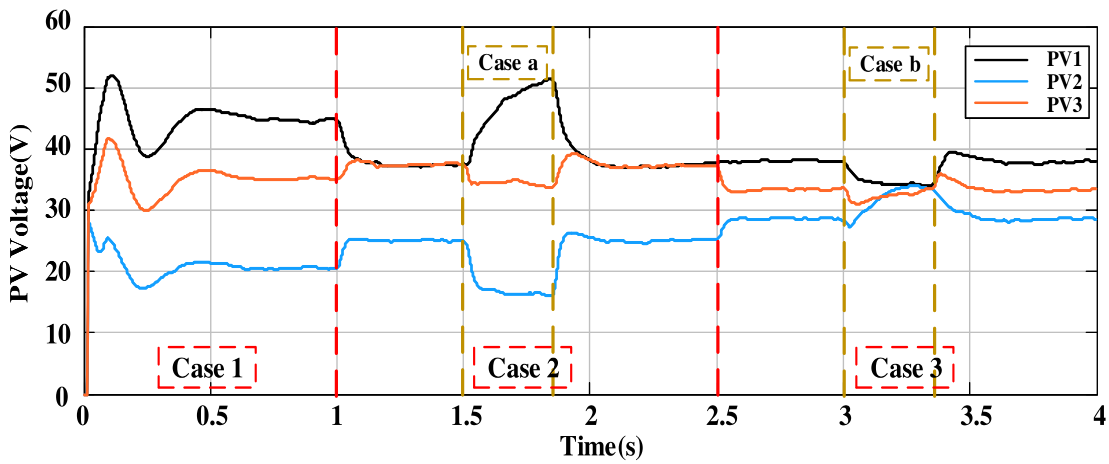
PV Voltage(V)
Time(s)
Case 1
Case 2
Case 3
Case a
Case b
PV1
PV2
PV3

(a) P&O

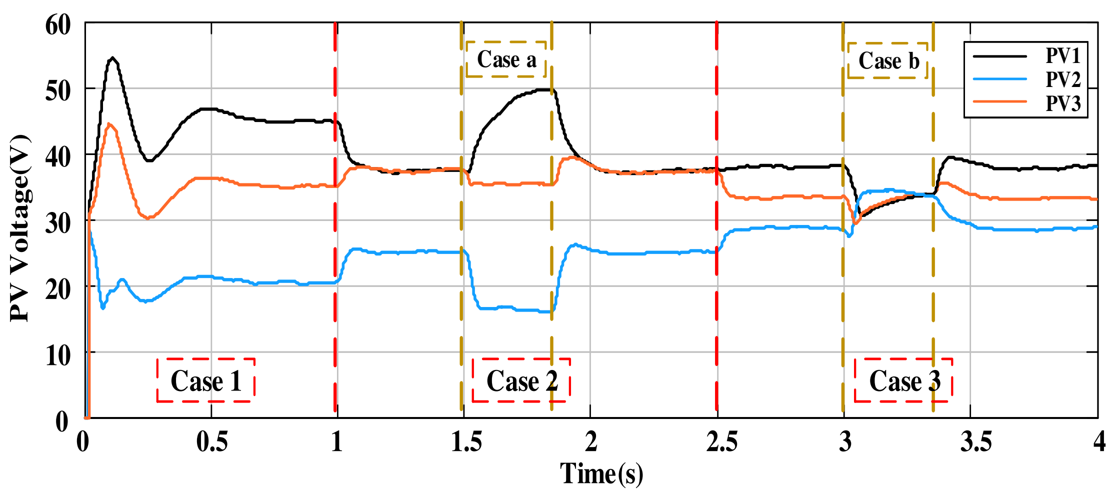
PV Voltage(V)
Time(s)
Case 1
Case 2
Case 3
Case a
Case b
PV1
PV2
PV3

(b)INC

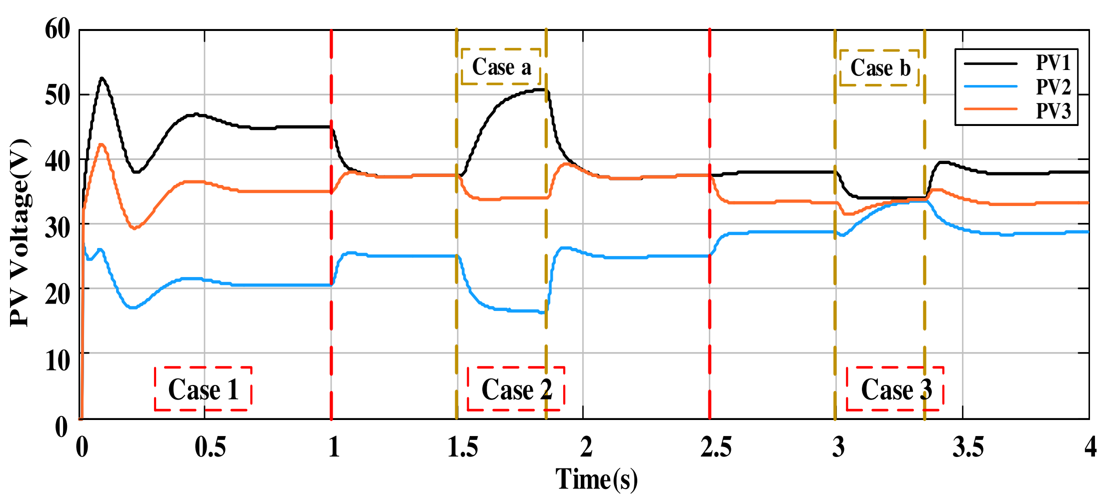
PV Voltage(V)
Time(s)
Case 1
Case 2
Case 3
Case a
Case b
PV1
PV2
PV3

(c) PSO

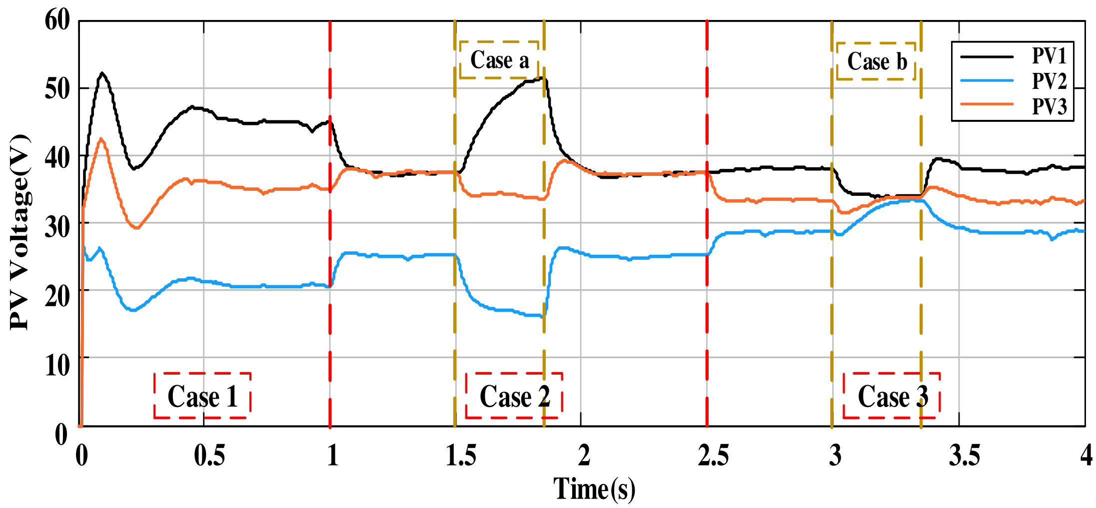

(d) ABC

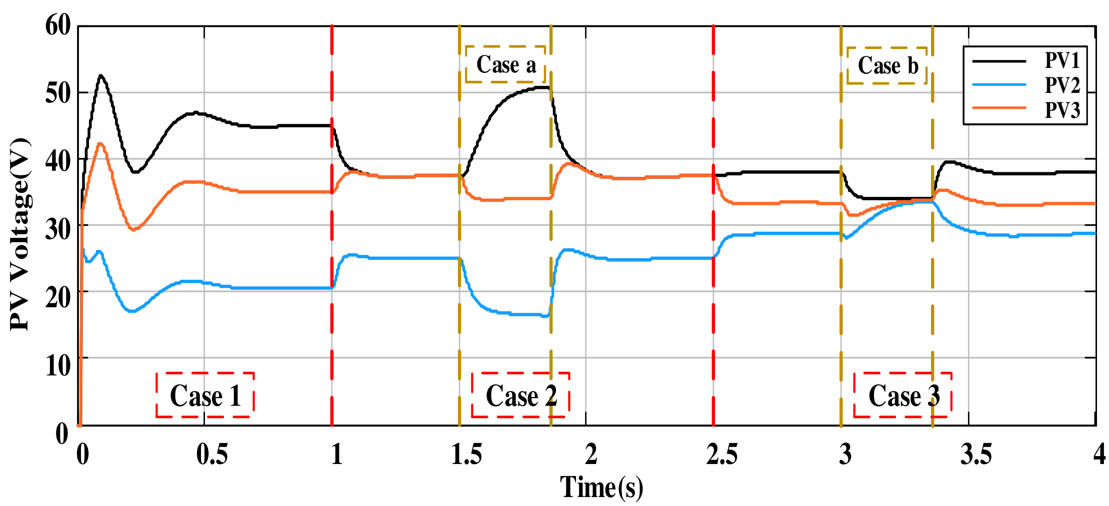

(e) SSA

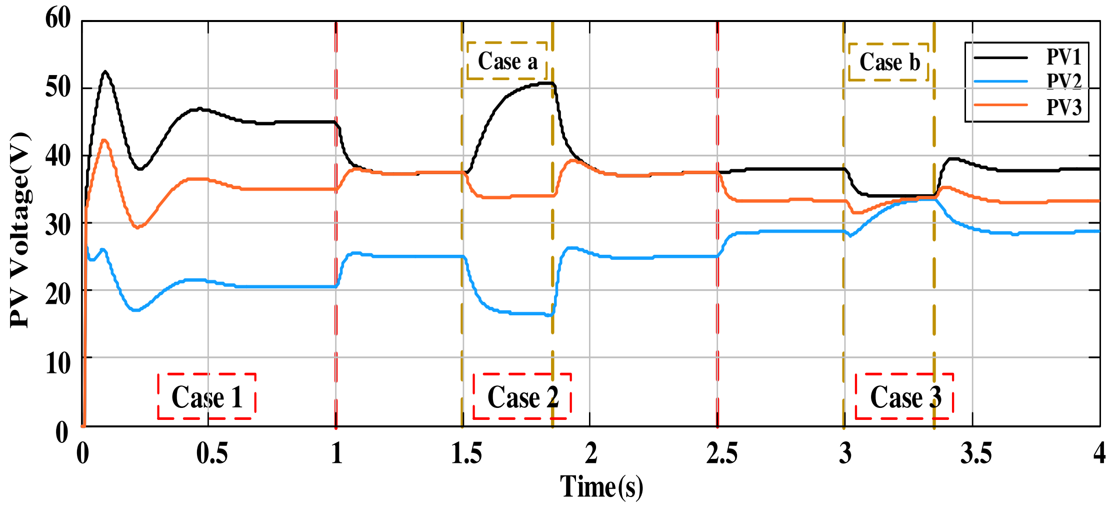
PV Voltage(V)
Time(s)
Case a
Case b
PV1
PV2
PV3
Case 1
Case 2
Case 3

(f) AFSA

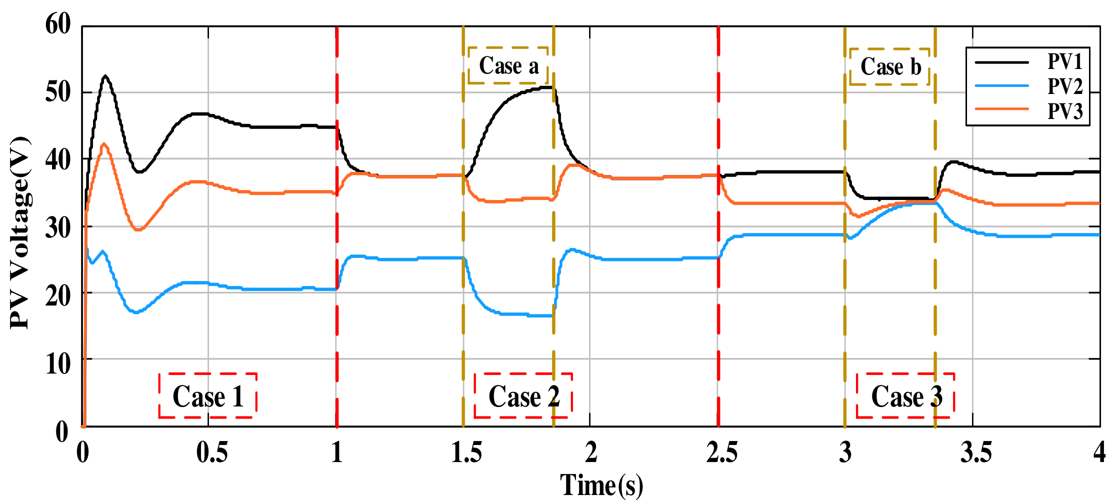
PV Voltage(V)
Time(s)
Case a
Case b
PV1
PV2
PV3
Case 1
Case 2
Case 3

(g) GWO

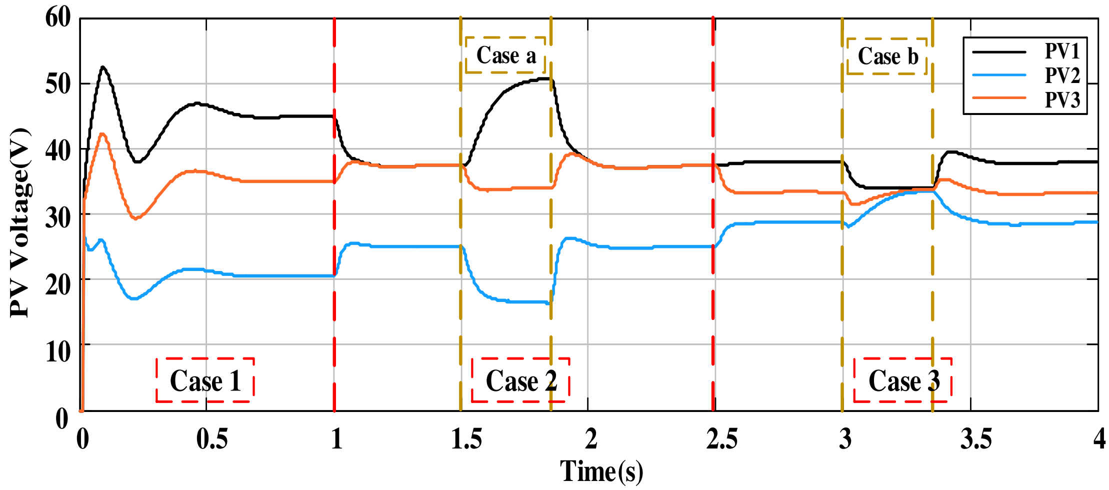

(h) SSAGWO

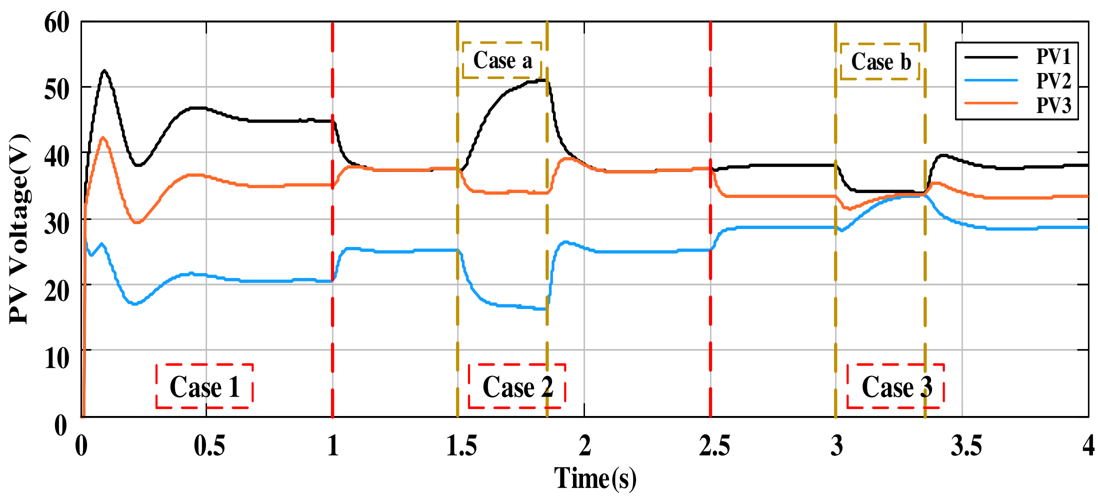

(i) SSAPSO

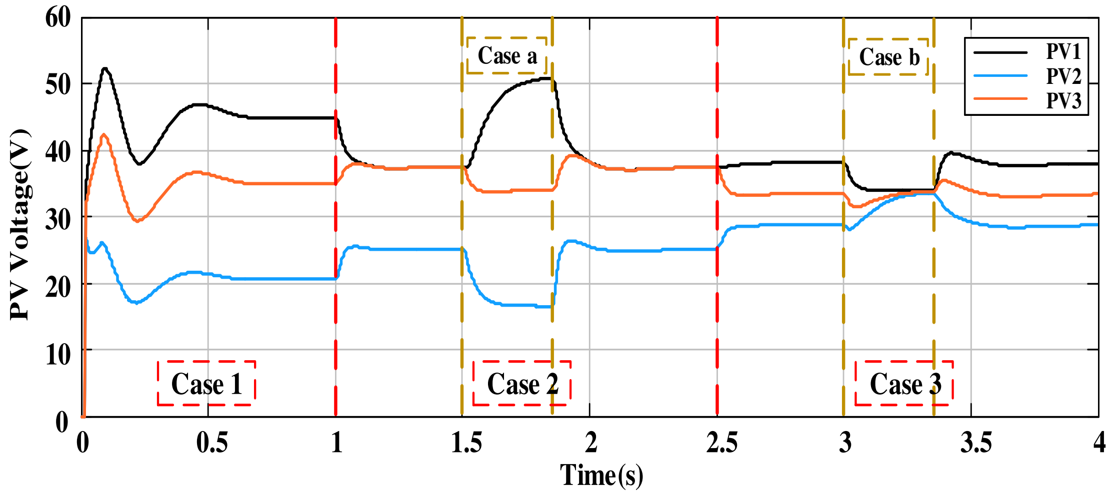

(j) DWSSA

Figure 10 Output voltage waveforms of each PV-converter measured by ten MPPT methods by (a) P&O, (b) INC, (c)PSO, (d)ABC, (e)SSA, (f) AFSA, (g) GWO, (h) SSAGWO, (i) SSAPSO, (j) DWSSA

The grid-side output current and voltage curves by DWSSA in the most severe fast-varying solar irradiation condition (Case 3) is shown in Figure 11(a). Figure 11(b)-(e) show the grid-side output current curves by the P&O, INC,SSA, PSO, ABC, AFSA, GWO, SSAGWA, SSAPSO and DWSSA methods under the fast-varying solar irradiation conditions (from Case 1 to Case 2, from Case 2 to Case 3, Case a and Case b). From Figure 11(b)-(c), it can be seen that the proposed DWSSA methodcan output higher current than the other methodsunder the two dynamicfast-varying solar irradiation cases, which also indicates that more generated power is harvested in the grid-connected system when the proposed DWSSA method is applied. In addition, Figure 11(d)-(e)show that the proposed DWSSA methodstill can keep the output current steady and highunder the sudden addition of Case a and Case b.

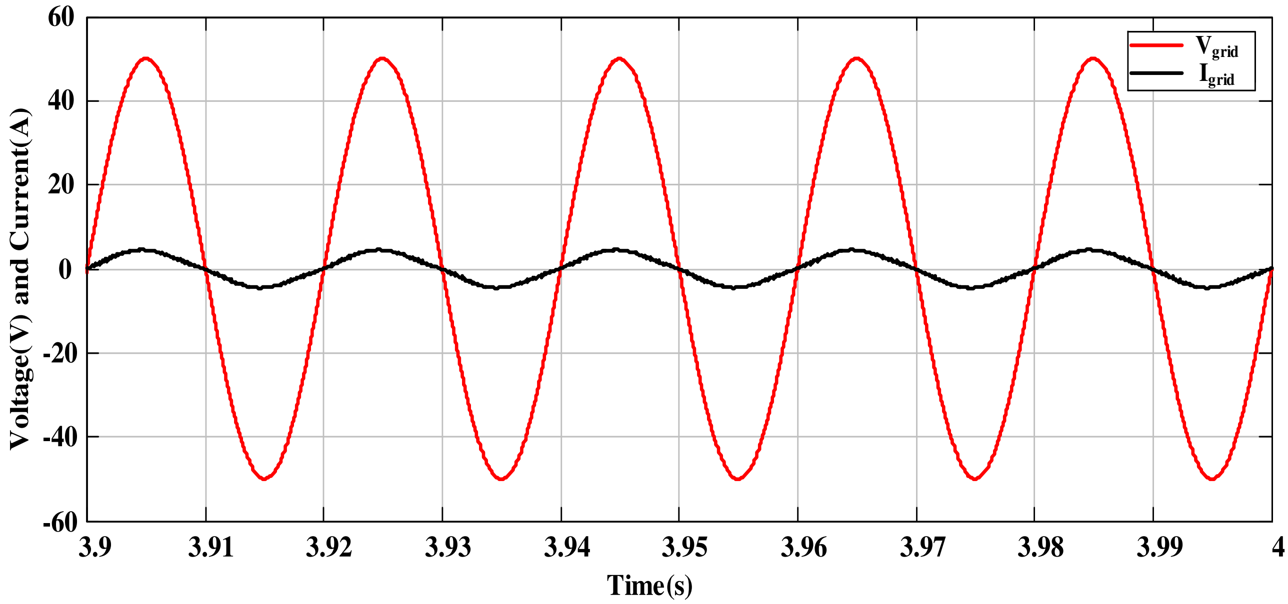
60
40
20
0
-20
-40
-60
Voltage(V) and Current(A)
3.9
3.91
3.92
3.93
3.94
3.95
3.96
3.97
3.98
3.99
4
Time(s)
V_{grid}
I_{grid}

(a)

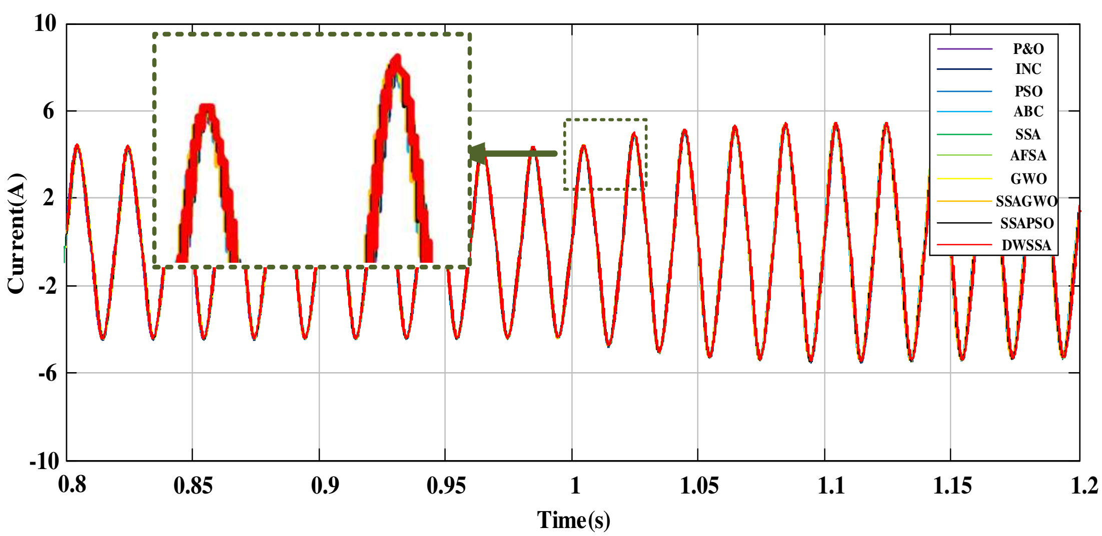
10
6
2
-2
-6
-10
Current(A)
0.8
0.85
0.9
0.95
1
1.05
1.1
1.15
1.2
Time(s)
P&O
INC
PSO
ABC
SSA
AFSA
GWO
SSAGWO
SSAPSO
DWSSA

(b)

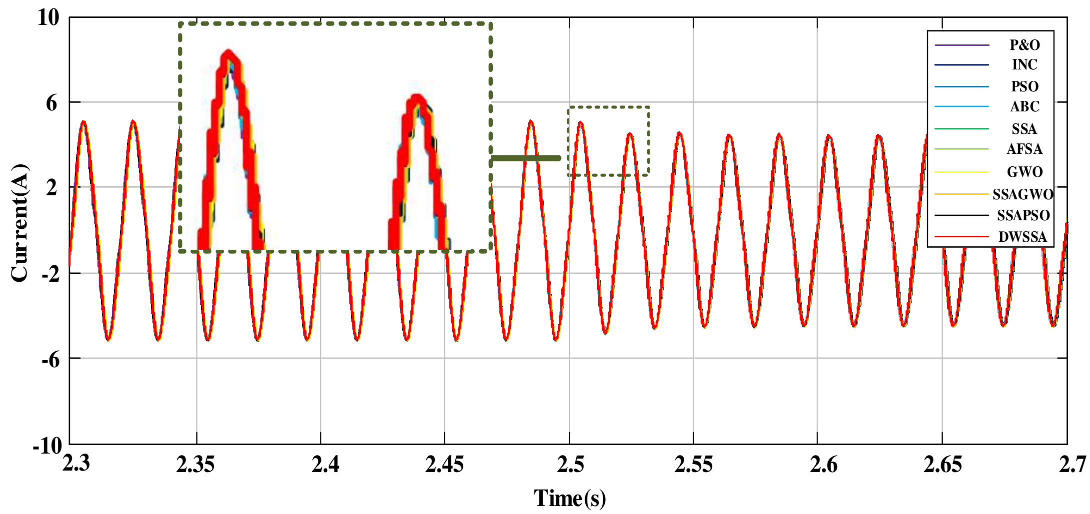
Current(A)
Time(s)
P&O
INC
PSO
ABC
SSA
AFSA
GWO
SSAGWO
SSAPSO
DWSSA

(c)

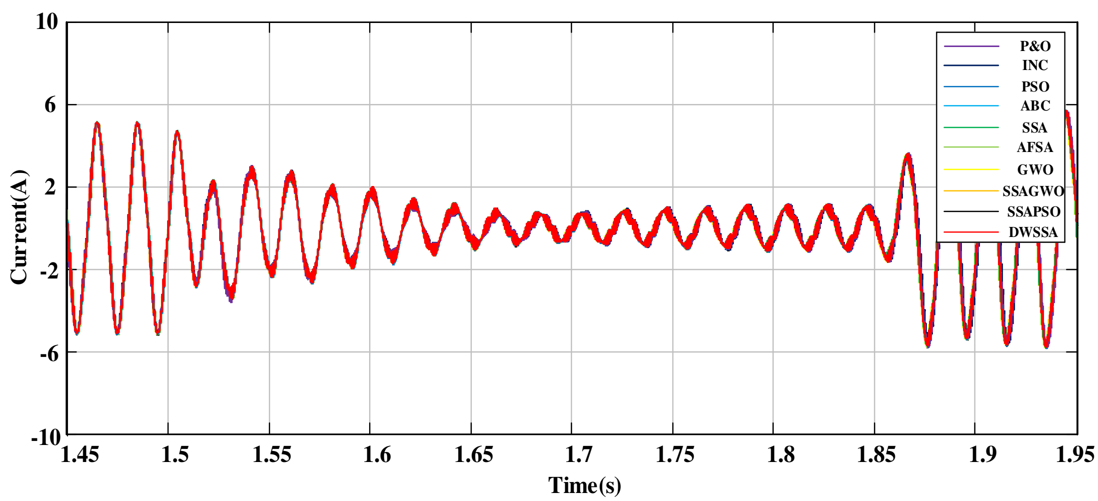
Current(A)
Time(s)
P&O
INC
PSO
ABC
SSA
AFSA
GWO
SSAGWO
SSAPSO
DWSSA

(d)

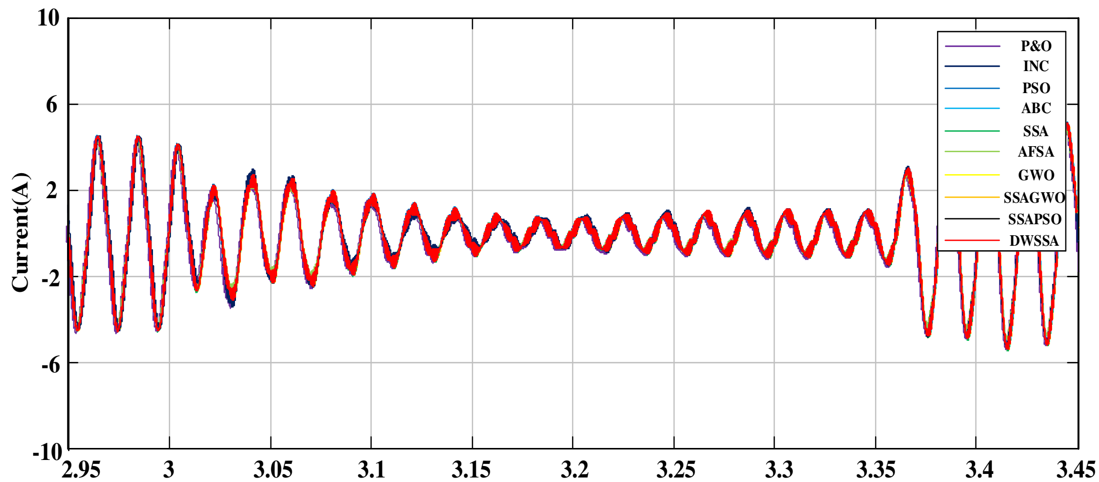

(e)

Figure 11Grid-side sinusoidal current and voltage curves under unity power factor control by ten MPPT methodsin differentsolar irradiation conditions: (a) Current and voltage curves by DWSSA (Case 3), (b) Current curves byten methods (from Case 1 to Case 2), (c) Current curvesby ten methods (from Case 2 to Case 3), (d) Current curvesby ten methods (Case a), (e) Current curvesby ten methods (Case b)

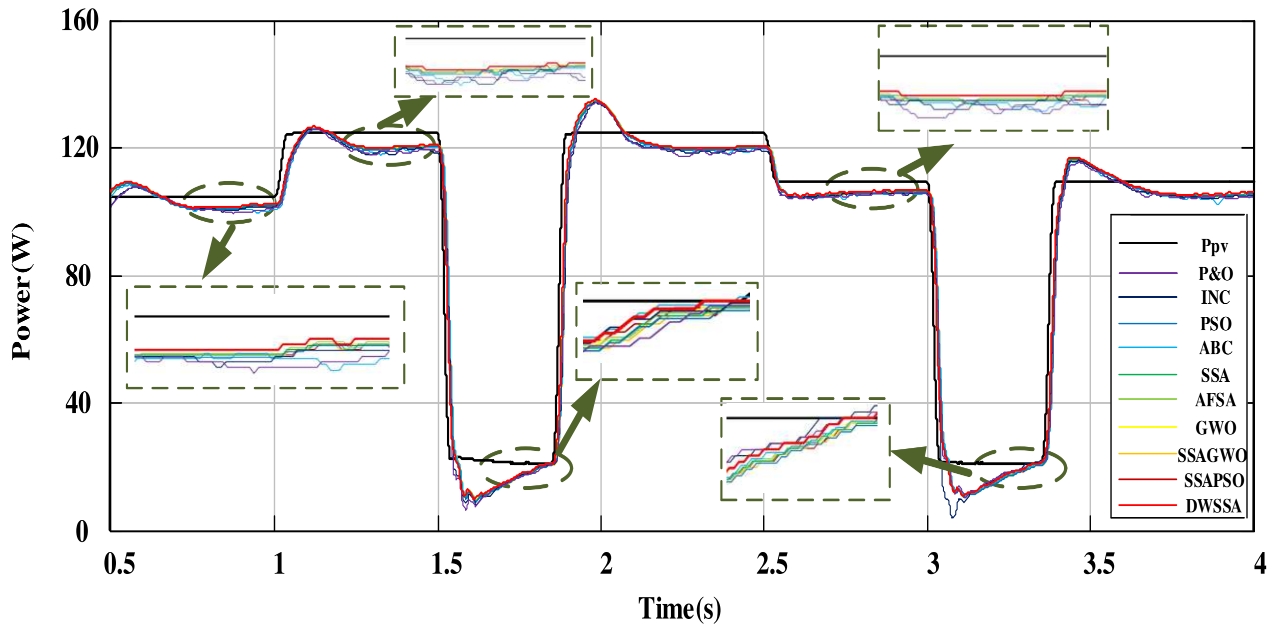

Figure 12 Output curves of the power delivered to grid under three cases, including sum of maximum power values found from the three sources (Ppv), P&O, INC, PSO, ABC, SSA, AFSA, GWO, SSAGWO, SSAPSO and DWSSA methods

Figure 12 shows the output power curves of the PV system based on 10 methods under the fast-varying solar irradiation conditions. The comprehensivequantitative comparison between the 10methods, including generated power (Power), power extraction percentage (Rate) and tracking timeto reach stability is summarized in Table 6. In Table 6, "--" represents that these algorithms can not reach stability in the given timeunder the sudden addition of Case a and Case b. Table 5 shows that the range of tracking time taken by the proposed DWSSA method is form 0.210s (minimum) to 0.761s (maximum) in five cases, which set the shortest duration between the fast-varying solar irradiation levels when the proposed PV system scheme with DWSSA method is used. From Figure 12 and Table 6, it can be seen that the tracking speed and accuracy of the proposed DWSSA method outperforms the other methods in most cases, especially, in Case 1 , Case a and Case b of the low solar irradiation level disturbances.More precisely, the power extraction percentage of the DWSSAmethod can be as high as 97.89% in Case 1, and the tracking time of the DWSSAmethodcan be as low as 0.316sunder the sudden addition of Case a.

Table 6 Output power exported to the grid by ten methods under the five cases

Method	Parameter	Case1	Case2	Casea	Case3	Caseb
	P_{pv}(W)	104.7	124.6	21.6	109.4	21.4
P&O	Power(W)	100.9	109.1	--	104.8	--
	Rate(%)	96.37	87.56	--	95.79	--
	Tracking Time(s)	0.769	0.339	--	0.100	--
INC	Power(W)	100.8	109.0	--	105	--
	Rate(%)	96.27	87.47	--	95.97	--
	Tracking Time(s)	0.755	0.251	--	0.130	--
PSO	Power(W)	102.3	121.0	20.5	106.3	--
	Rate(%)	97.71	97.11	94.91	97.16	--
	Tracking Time(s)	0.795	0.300	0.312	0.226	--
ABC	Power(W)	101.8	120.7	20.9	105.8	20.5
	Rate(%)	97.23	96.86	96.75	96.70	95.79
	Tracking Time(s)	0.765	0.280	0.319	0.315	0.335
SSA	Power(W)	102.3	121.0	20.5	106.4	20.6

	Rate(%)	97.70	97.11	95.34	97.25	96.26
	Tracking Time(s)	0.783	0.281	0.321	0.251	0.326
AFSA	Power(W)	102.2	121.1	20.4	106.3	20.97
	Rate(%)	97.61	97.19	94.44	97.16	97.99
	Tracking Time(s)	0.787	0.297	0.317	0.239	0.339
GWO	Power(W)	102.2	121.0	20.9	106.4	20.8
	Rate(%)	97.61	97.11	96.75	97.25	97.19
	Tracking Time(s)	0.782	0.279	0.34	0.217	0.326
SSAGWO	Power(W)	102.3	121.1	20.9	106.5	20.8
	Rate(%)	97.71	97.19	96.75	97.34	97.19
	Tracking Time(s)	0.777	0.336	0.341	0.33	0.326
SSAPSO	Power(W)	102.0	121.1	20.7	106.4	20.7
	Rate(%)	97.42	97.19	95.83	97.34	96.72
	Tracking Time(s)	0.790	0.300	0.32	0.34	0.33
DWSSA	Power(W)	102.5	121.2	21	106.6	20.8
	Rate(%)	97.89	97.29	97.22	97.44	97.19
	Tracking Time(s)	0.761	0.290	0.316	0.210	0.332

4 Conclusions

In this paper, a novelgrid-connected PV systemconfiguration composed ofthe multilevel cascaded PV boost converter unitswith the novel DWSSA controller and anANPC inverter has been proposed. Different from the conventional PV systemconfiguration, besides one ANPC inverter used to connect to the ac grid, the convergence and stability of MPPT controller is adequately considered to overcome the fast-varying solar irradiation conditionsand extract maximum power exploitation from the PV system.The mathematical model of the proposed configuration has beenestablished. Moreover, the Lyapunov theoryhas been utilised to verify the stability of the proposed DWSSA algorithm and the algorithm convergence has been also investigated on two representative sets of benchmarktest functions. The final numerical simulation and establishedtest platformsimulation validates that the proposed DWSSA algorithm has faster convergence speed and higher stability, which enables the proposed PV system to maintain high energy extraction efficiencyunder the different solar irradiation levels.The power extraction percentage of the proposed DWSSAmethod can be as high as 97.89% under the most severe PSCs. Moreover, the proposed PV system still has a good performance on it when the stochastic disturbances of low solar irradiation levels are added.

In future work, there are still some problems need to be valued. On the one hand, although the dynamic *w* factor introduced into the proposed MPPT algorithm can track the maximum power point quickly and effectivelyand overcomes the power loss caused be the fast-varying solar irradiation levelsto some extent, the output voltage and power is not smooth enough. On the other hand, the tracking stability time is a little longer in rare cases,especially after the sudden addition of low solar irradiation level disturbance. Hence, the correction and improvement for the sensitivity of the dynamic *w* factorneeds to be studied further.Additionally, we will continue to study on the simulation verification of the proposed PV system configuration based on hardware platform in the future work.

Acknowledgements

This work has been supported by the China Postdoctoral Science Foundation (Grant No. 2018M643410), the Chongqing Special Postdoctoral Science Foundation (Grant No. XmT2018033), the Natural Science FoundationPostdoctoral Science Foundation of Chongqing, China (Grant No. cstc2019jcyj-bshX0047), the National Natural Science Foundation of China (Grant No. 51707026) and the National Key Research and Development Program (Grant No. 2018YFB0905802).

Appendix A

The description of 23 benchmark functions is shown in the table below.

Name	Function	Dim	Search range	f_{min}	Type
Sphere	$f_1 = \sum_{i=1}^{n} x_i^2$	30	[-100, 100]	0	Unimodal
Schwefel 2.22	$f_2 = \sum_{i=1}^{n} \lvert x_i \rvert + \prod_{i=1}^{n} \lvert x_i \rvert$	30	[-10, 10]	0	
Schewefel 1.2	$f_3 = \sum_{i=1}^{n} \left(\sum_{j-1}^{i} x_j \right)^2$	30	[-100, 100]	0	
Schewefel 2.21	$f_4 = \max_i \{ \lvert x_i \rvert, 1 \le i \le n \}$	30	[-100, 100]	0	
Generalized Rosenbrock	$f_5 = \sum_{i=1}^{n-1} \left[100 \left(x_{i+1} - x_i^2 \right)^2 + \left(x_i - 1 \right)^2 \right]$	30	[-30, 30]	0	
Step	$f_6 = \sum_{i=1}^{n} \left(\left[x_i + 0.5 \right] \right)^2$	30	[-100,100]	0	

Quartic	$f_7 = \sum_{i=1}^{n} i x_i^4 + random\left[0,1\right)$	30	[-1.28,1.28]	0	
Generalized Schwefel's Problem 2.26	$f_8 = \sum_{i=1}^{n} -x_i \sin\left(\sqrt{\lvert x_i \rvert}\right)$	30	[-500,500]	-418.9829×5	
Generalized Rastrigin	$f_9 = \sum_{i=1}^{n}\left[x_i^2 - 10\cos\left(2\pi x_i\right) + 10\right]$	30	[-5.12, 5.12]	0	
Ackley	$f_{10} = -20\exp\left(-0.2\sqrt{\frac{1}{n}\sum_{i=1}^{n} x_i^2}\right) - \exp\left(\frac{1}{n}\sum_{i=1}^{n}\cos\left(2\pi x_i\right)\right) + 20 + e$	30	[-32, 32]	0	
Generalized Griewank	$f_{11} = \frac{1}{4000}\sum_{i=1}^{n} x_i^2 - \prod_{i=1}^{n}\cos(\frac{x_i}{\sqrt{i}}) + 1$	30	[-600, 600]	0	Multimodal
Generalized Penalized	$f_{12} = \frac{\pi}{n}\left\{10\sin(\pi y_1) + \sum_{i=1}^{n-1}(y_i - 1)^2\left[1 + 10\sin^2(\pi y_{i+1})\right] + \left(y_n - 1\right)^2\right\}$ $+\sum_{i=1}^{n} u\left(x_i, 10, 100, 4\right)$ $y_i = 1 + \frac{x_i + 1}{4}$ $u(x_i, a, k, m) = \begin{cases} k(x_i - a)^m & x_i > a \\ 0 & -a < x_i < a \\ k(x_i - a)^{-m} & x_i < -a \end{cases}$	30	[-50, 50]	0	
Generalized Penalized	$f_{13} = 0.1\left\{\sin^2\left(3\pi x_1\right) + \sum_{i=1}^{n}\left(x_i - 1\right)^2\left[1 + \sin^2\left(3\pi x_1 + 1\right)\right] + \left(x_n - 1\right)^2\left[1 + \sin^2\left(2\pi x_n\right)\right]\right\}$ $+\sum_{i=1}^{n} u(x_i, 5100, 4)$	30	[-50, 50]	0	
Shekel's Foxholes	$f_{14} = (\frac{1}{500} + \sum_{j=1}^{25}\frac{1}{j + \sum_{i=1}^{2}(x_i - a_{ij})^6})^{-1}$	2	[-65, 65]	1	
Kowalik	$f_{15} = \sum_{i=1}^{11}\left[a_i - \frac{x_1(b_i^2 + b_i x_2)}{b_i^2 + b_i x_3 + x_4}\right]^2$	4	[-5, 5]	0.00030	
Six-Hump Camel-Back	$f_{16} = 4x_1^2 - 2.1x_1^4 + \frac{1}{3}x_1^6 + x_1 x_2 - 4x_2^2 + 4x_2^4$	2	[-5, 5]	-1.0316	
Branin	$f_{17} = (x_2 - \frac{5.1}{4\pi^2}x_1^2 + \frac{5}{\pi}x_1 - 6)^2 + 10(1 - \frac{1}{8\pi})\cos x_1 + 10$	2	[-5, 5]	0.398	Fixed-dimenstion
Goldstein-Price	$f_{18} = \left[1 + (x_1 + x_2 + 1)^2(19 - 14x_1 + 3x_1^2 - 14x_2 + 6x_1x_2 + 3x_2^2)\right]$ $\times\left[30 + (2x_1 - 3x_2)^2 \times (18 - 32x_1 + 12x_1^2 + 48x_2 - 36x_1x_2 + 27x_2^2)\right]$	2	[-2, 2]	3	Multimodal
Hartman's Family	$f_{19} = -\sum_{i=1}^{4} c_i \exp(-\sum_{j=3}^{3} a_{ij}(x_j - p_{ij})^2)$	3	[1, 3]	-3.86	
Hartman's Family	$f_{20} = -\sum_{i=1}^{4} c_i \exp(-\sum_{j=3}^{6} a_{ij}(x_j - p_{ij})^2)$	6	[0, 1]	-3.32	
Shekel's Family	$f_{21} = -\sum_{i=1}^{5}\left[\left(X - a_i\right)\left(X - a_i\right)^T + c_i\right]^{-1}$	4	[0, 10]	-10.1532	

Shekel's Family	$f_{22} = -\sum_{i=1}^{7}\left[\left(X-a_i\right)\left(X-a_i\right)^T + c_i\right]^{-1}$	4	[0, 10]	-10.4028
Shekel's Family	$f_{23} = -\sum_{i=1}^{10}\left[\left(X-a_i\right)\left(X-a_i\right)^T + c_i\right]^{-1}$	4	[0, 10]	-10.5363

Appendix B

The results comparison of the 13 algorithms on 23 functions is shown in the table below.

Fun	Index	PSO	AFSA	SSA	SSAPSO	ABC	ALO	DA	GOA	MFO	MVO	SCA	SSA-GWO	DWSSA
	Best	2.2710e+02	5.6046e-08	1.2704e-08	4.7039e-05	1.0883e+02	**0**	7.1678e+01	**0**	2.7751e-01	4.9239e-01	**0**	5.4386e-10	2.8636e-24
f_1	Mean	6.9953e+02	2.3309e-05	2.2939e-08	3.0646e-03	2.4711e+02	1.1216e-04	9.3251e+02	4.0715e+00	1.0016e+03	7.8044e-01	2.4443e+00	1.0672e-09	**7.1296e-24**
	STD	3.2148e+02	2.9373e-05	1.0072e-08	7.1797e-03	9.4346e+01	3.651e-05	7.7379e+02	2.9630e+00	3.0776e+03	2.1578e-01	3.0617e+00	3.0463e-10	**3.9986e-24**
	Time/s	0.141785	6.958637	0.284591	0.349432	0.065042	31.441462	53.528572	141.369355	0.202590	0.357421	0.210181	0.286691	0.282894
	Best	9.5592e+00	1.2265e-04	3.6776e-03	2.6424e-01	1.1759e+00	**0**	1.5477e+00	**0**	2.0948e-01	3.4724e-01	**0**	1.2613e-05	8.9464e-13
f_2	Mean	1.9460e+01	1.6827e-03	1.2611e+00	1.9449e+00	1.7720e+00	4.6117e+01	1.0848e+01	5.0470e+00	3.6179e+01	5.9075e-01	7.6463e-03	1.2655e-04	**1.1939e-12**
	STD	8.3389e+00	1.7032e-03	1.9181e+00	1.2493e+00	3.0487e-01	5.0070e+01	5.7567e+00	2.6464e+00	2.0291e+01	1.7967e-01	7.5381e-03	3.2553e-04	**2.0440e-13**
	Time/s	0.145467	7.075559	0.289579	0.335695	0.067691	31.424016	44.377439	143.908003	0.214059	0.327568	0.217141	0.298623	0.285275
	Best	8.6650e+02	2.1917e-06	2.1249e+02	1.0765e+02	2.3311e+04	**0**	5.1645e+02	**0**	3.5647e+03	3.8037e+01	**0**	1.5475e+02	1.4134e-23
f_3	Mean	2.0490e+03	1.8003e-02	5.6948e+02	4.9422e+02	2.8248e+04	1.8500e+03	7.6980e+03	1.6340e+03	1.7516e+04	9.6848e+01	6.9793e+03	5.8766e+02	**4.8492e-23**
	STD	9.5750e+02	3.9473e-02	3.6011e+02	3.8694e+02	4.6685e+03	1.1997e+03	6.2012e+03	8.7565e+02	1.1693e+04	3.4373e+01	5.2679e+03	3.5338e+02	**3.498e-23**
	Time/s	1.039173	35.184749	0.703437	1.006196	0.481177	31.055538	44.349288	138.938919	0.594835	0.812523	0.656634	0.697743	0.688248
	Best	1.3180e+01	6.4124e-06	2.6123e+00	2.6708e+00	5.6444e+01	**0**	1.3235e+01	**0**	4.5896e+01	6.4528e-01	**0**	1.0145e-02	5.8875e-13
f_4	Mean	1.7073e+01	4.8700e-04	7.7924e+00	7.0336e+00	6.9111e+01	1.3173e+01	2.3798e+01	8.2111e+00	5.8621e+01	1.2285e+00	2.7034e+01	4.3348e-01	**1.0023e-12**
	STD	2.2537e+00	6.1559e-04	3.2619e+00	2.4171e+00	5.1269e+00	5.1133e+00	7.3265e+00	2.7319e+00	8.5405e+00	3.7424e-01	1.0180e+01	5.2284e-01	**2.2971e-13**
	Time/s	0.144502	7.219804	0.292976	0.341741	0.075903	32.304085	64.250967	144.176631	0.207027	0.372066	0.229473	0.306532	0.298173
	Best	6.9280e+03	2.9922e-08	2.6580e+01	2.7666e+01	3.5541e+03	**0**	3.0295e+03	**0**	1.9928e+02	2.7846e+01	**0**	2.6294e+01	2.8443e+01
f_5	Mean	6.5520e+04	**2.0666e-04**	1.8666e+02	1.7558e+02	3.6844e+04	2.1657e+02	9.6142e+04	4.5770e+02	9.5810e+03	2.8692e+02	1.2376e+04	7.2092e+01	2.8512e+01
	STD	4.5489e+04	**4.3062e-04**	3.0970e+02	1.9025e+02	4.2091e+04	3.9971e+02	1.3575e+05	3.9757e+02	2.7614e+04	5.3441e+02	1.6456e+04	1.0667e+02	3.4592e-02
	Time/s	0.245931	10.435942	0.346163	0.419811	0.107532	31.345550	33.691516	146.519216	0.259394	0.410578	0.279400	0.450861	0.335162
	Best	2.2729e+02	7.259e-12	1.3005e-08	3.7647e-05	8.3096e+01	**0**	2.8043e+01	**0**	4.7645e-01	3.6757e-01	**0**	1.3293e-08	1.2352e-08
f_6	Mean	8.0818e+02	4.9793e-05	**1.8919e-08**	2.3638e-03	3.6875e+02	1.1925e-04	5.8589e+02	3.9216e+00	2.0219e+03	6.9552e-01	8.0663e+00	2.393e-08	1.9893e-08
	STD	2.9162e+02	1.2162e-04	**3.6379e-09**	4.2521e-03	2.50003e+02	7.8378e-05	5.7197e+02	2.9158e+00	5.2833e+03	1.7012e-01	5.8813e+00	5.5584e-09	4.6758e-09
	Time/s	0.149269	6.923988	0.296949	0.343559	0.062538	31.272797	34.899824	139.403127	0.209892	0.367938	0.209685	0.275083	0.285884
	Best	1.2625e-01	1.0153e-04	4.9819e-02	8.4075e-02	4.0026e-01	**0**	2.8332e-02	**0**	4.6706e-02	6.8940e-03	**0**	7.9227e-03	2.0277e-06
f_7	Mean	7.2918e-01	1.2538e-01	9.0076e-02	6.5132e-01	7.6679e-01	1.2221e-01	2.7239e-01	2.8510e-02	2.5644e+00	2.4090e-02	4.8755e-02	2.5193e-02	**5.6015e-05**
	STD	2.5659e-01	2.3922e-01	3.2866e-02	3.8693e-01	2.0921e-01	4.8896e-02	2.1534e-01	1.2472e-02	4.4934e+00	1.1691e-02	4.4348e-02	1.2462e-02	**6.1415e-05**
	Time/s	0.465193	14.279351	0.398296	0.529126	0.181314	29.006535	30.122431	127.432943	0.319866	0.450440	0.326102	0.461451	0.395998
	Best	-4.164e+182	-1.257e+04	-9.761e+03	-7.55e+209	-9.0717e+03	-8.621e+03	-7.140e+03	-9.419e+03	-9.988e+03	-8.935e+03	**-4.440e+03**	-8.226e+03	-9.078e+03
f_8	Mean	-2.082e+181	-1.257e+04	-7.678e+03	-3.78e+208	-8.455e+03	-5.709e+03	-5.597e+03	-7.622e+03	8.968e+03	-8.063e+03	**-3.907e+03**	-7.584e+03	-7.236e+03
	STD	Inf	6.1360e-04	8.8823e+02	Inf	3.9719e+02	7.9195e+02	5.9097e+02	6.7914e+02	7.7527e+02	5.0386e+02	**2.9490e+02**	5.2857e+02	9.6582e+02
	Time/s	0.648524	10.020902	0.345646	0.635834	0.117216	30.962516	47.256799	137.400566	0.249565	0.291892	0.265278	0.360470	0.333487
	Best	6.9337e+01	3.426e-10	2.0894e+01	2.7859e+01	4.7603e+01	**0**	4.8434e+01	**0**	8.5609e+01	5.8055e+01	**0**	1.1940e+01	**0**
f_9	Mean	9.4055e+01	2.7258e-06	4.2783e+01	5.4524e+01	7.2213e+01	6.6563e+01	1.3910e+02	7.6309e+01	1.4420e+02	1.1120e+02	2.9753e+01	3.7460e+01	**0**
	STD	1.8665e+01	5.8448e-06	1.6696e+01	1.6065e+01	1.3975e+01	1.8065e+01	3.4889e+01	2.4535e+01	3.7046e+01	2.9301e+01	2.4409e+01	1.6423e+01	**0**
	Time/s	0.206943	8.441158	0.329852	0.375400	0.103340	34.083204	107.439530	148.991639	0.233922	0.422455	0.241634	0.328060	0.313610
	Best	7.2611e+00	2.4989e-05	4.9876e-01	3.0481e-01	7.6173e+00	**0**	2.9763e+00	**0**	4.3284e-01	3.2378e-01	**0**	9.6768e-06	4.5919e-13
f_{10}	Mean	9.697e+00	9.7098e-04	2.0103e+00	2.253e+00	1.0019e+01	2.2851e+00	7.5932e+00	3.5461e+00	1.2410e+01	1.2811e+00	1.223e+01.	1.8182e+00	**6.5459e-13**
	STD	1.5985e+00	8.0984e-04	4.6941e-01	7.9293e-01	1.4655e+00	6.5668e-01	2.5600e+00	1.3259e+00	8.4555e+00	7.3056e-01	9.6887e+00	6.3035e-01	**1.386e-13**
	Time/s	0.238131	9.191787	0.360968	0.415970	0.106129	34.698850	38.228427	158.761179	0.267640	0.446533	0.272692	0.354253	0.335799
	Best	3.539e+00	2.2815e-08	6.7822e-06	3.0822e-03	1.7406e+00	**0**	1.2638e+00	**0**	1.9804e-01	4.3939e-01	**0**	8.6622e-10	**0**
f_{11}	Mean	7.5336e+00	5.5589e-05	1.4786e-02	3.3110e-02	3.5334e+00	2.5318e-02	6.0483e+00	6.1132e-01	9.752e+00	7.4964e-01	7.6026e-01	3.7402e-04	**0**
	STD	2.0911e+00	7.7124e-05	1.2207e-02	3.2389e-02	1.493e+00	2.2802e-02	2.8437e+00	1.4745e-01	2.7724e+01	1.1383e-01	3.4756e-01	1.6726e-03	**0**
	Time/s	0.339329	13.468534	0.390799	0.487929	0.151555	34.160061	40.197396	153.725296	0.311677	0.505367	0.311472	0.415154	0.382262
	Best	8.1678e+00	9.7726e-11	1.6574e+00	1.1362e+00	8.5891e-01	**0**	3.1697e+00	**0**	2.5093e-01	2.0961e-01	**0**	1.8921e-02	3.5904e-08
f_{12}	Mean	1.4470e+01	**3.5144e-07**	4.8677e+00	5.1599e+00	2.1500e+00	9.9056e+00	3.7606e+02	5.9956e+00	3.3263e+00	1.5420e+00	1.9746e+04	6.1867e-01	1.5002e-04
	STD	6.7460e+00	**8.5327e-07**	2.4379e+00	2.7990e+00	9.4344e-01	3.3953e+00	1.5783e+03	2.7787e+00	2.5831e+00	8.0562e-01	8.8233e+04	4.1662e-01	2.9822e-04
	Time/s	1.121484	36.481564	0.721823	0.997138	0.505110	31.923030	52.129852	139.978854	0.647011	0.768647	0.650420	1.011977	0.711814
	Best	3.8672e+01	1.2408e-08	4.0699e-07	4.8862e-02	3.3703e+00	**0**	1.0907e+01	**0**	2.1269	5.8937e-02	**0**	2.472e-07	1.9925e-05
f_{13}	Mean	4.9518e+02	**5.0089e-06**	4.3813e+00	1.3627e+01	3.3097e+01	7.1856e+00	1.7484e+04	1.0966e+01	1.2891e+01	1.2119e-01	8.8988e+02	2.1062e-02	2.0832e+00
	STD	8.0385e+02	**9.0584e-06**	8.9967e+00	1.4560e+01	6.3515e+01	1.6720e+01	5.6606e+04	1.2928e+01	1.7264e+01	4.0630e-02	3.7803e+03	6.1821e-02	1.3887e+00
	Time/s	1.138841	36.167332	0.719741	0.979475	0.513161	31.373295	35.245279	141.455617	0.632449	0.794044	0.650372	1.000066	0.708050
	Best	**9.9800e-01**	**9.9800e-01**	**9.9800e-01**	**9.9800e-01**	**9.9800e-01**	0	**9.9800e-01**	**9.9800e-01**	**9.9800e-01**	**9.9800e-01**	0	**9.9800e-01**	**9.9800e-01**
f_{14}	Mean	**9.9800e-01**	**9.9801e-01**	**9.9800e-01**	**9.9800e-01**	**9.9800e-01**	1.7889e+00	**9.9800e-01**	**9.9800e-01**	1.2962e+00	**9.9800e-01**	1.1964e+00	**9.9800e-01**	1.0974e+00
	STD	**0**	9.4140e-06	1.2820e-16	1.6550e-16	1.8130e-16	1.5980e+00	3.7581e-11	2.3984e-16	4.8016e-01	7.4069e-12	6.2742e-01	1.887e-16	3.1434e-01
	Time/s	4.215155	139.720811	2.410537	3.657259	2.158394	9.482979	42.350683	21.609230	2.241188	2.349810	2.203469	2.327133	2.321079
	Best	**3.0749e-04**	**3.3632e-04**	5.4982e-04	**3.0749e-04**	3.2904e-04	**3.0749e-04**	7.2069e-04	**3.0749e-04**	6.8162e-04	4.4093e-04	**3.0749e-04**	3.9371e-04	**3.0749e-04**
f_{15}	Mean	8.8123e-04	9.3783e-04	9.0978e-04	1.2171e-03	7.2498e-04	7.8388e-04	2.4419e-03	1.4795e-02	8.4999e-04	3.2176e-03	9.7397e-04	9.0295e-04	**3.7210e-04**
	STD	2.3318e-04	4.7870e-04	2.4584e-04	3.6762e-04	1.3467e-04	**1.1809e-04**	4.2521e-03	1.8926e-02	2.3909e-04	6.2927e-03	3.9758e-04	2.5572e-04	2.0264e-04
	Time/s	0.147041	7.264158	0.213881	0.201506	0.070441	4.847709	66.957110	18.840282	0.113410	0.157194	0.113541	0.212607	0.198785
	Best	**-1.0316**	**-1.0316**	**-1.0316**	**-1.0316**	**-1.0316**	**-1.0316**	**-1.0316**	**-1.0316**	**-1.0316**	**-1.0316**	**-1.0316**	**-1.0316**	**-1.0316**
f_{16}	Mean	**-1.0316**	**-1.0316**	**-1.0316**	**-1.0316**	**-1.0316**	**-1.0316**	**-1.0316**	**-1.0316**	**-1.0316**	**-1.0316**	**-1.0316**	**-1.0316**	**-1.0316**
	STD	**2.1612e-16**	6.2631e-07	3.788e-14	6.8624e-15	3.4121e-08	1.044e-13	1.1161e-07	4.8093e-13	2.2781e-16	2.6292e-07	1.9834e-05	3.4682e-14	2.0401e-14
	Time/s	0.119909	5.473484	0.169035	0.191447	0.059631	2.511533	14.019795	9.632421	0.090958	0.116695	0.083128	0.176911	0.162562
	Best	**0.39789**	**0.39986**	**0.39789**	**0.39789**	**0.39789**	**0.39789**	**0.39789**	**0.39789**	**0.39789**	**0.39789**	**0.39789**	**0.39789**	**0.39789**
f_{17}	Mean	**0.39789**	0.41829	**0.39789**	**0.39789**	**0.39789**	**0.39789**	**0.39789**	**0.39789**	**0.39789**	**0.39789**	0.39832	**0.39789**	**0.39789**
	STD	**0**	1.8295e-02	7.9879e-15	5.3591e-04	5.5609e-15	9.8584e-15	3.763e-12	2.5182e-13	**0**	1.307e-07	4.1125e-04	1.2873e-14	1.3838e-14
	Time/s	0.099430	5.417444	0.181203	0.145829	0.048592	2.492936	15.994788	9.724662	0.087226	0.124158	0.083793	0.173162	0.162603
f_{18}	Best	**3**	**3**	**3**	**3**	**3**	**3**	**3**	**3**	**3**	**3**	**3**	**3**	**3**

	Mean	**3**	**3**	**3**	**3**	**3**	**3**	**3**	**3**	**3**	**3**	**3**	**3**	**3**
	STD	1.3047e-15	5.1074e-07	1.9288e-13	6.6532e-14	2.2111e-15	1.6044e-13	6.8856e-12	4.2823e-12	**9.7188e-16**	1.3037e-06	2.7095e-05	3.4655e-13	3.4333e-13
	Time/s	0.091075	4.987683	0.164198	0.157228	0.059217	2.432624	20.590036	9.635613	0.083503	0.118338	0.074470	0.177384	0.162694
f_{19}	Best	-3.2398	-0.30048	-0.30048	-3.3588	**-3.4576**	-0.30048	-0.30048	-0.30048	-0.30048	-0.30048	-0.30048	-0.30048	-0.30048
	Mean	Inf	-0.30048	-0.30048	-2.4197	**-2.6073**	-0.30048	-0.30048	-0.30048	-0.30048	-0.30048	-0.30048	-0.30048	-0.30048
	STD	NaN	**1.1391e-16**	**1.1391e-16**	6.5931e-01	5.1568e-01	**1.1391e-16**	**1.1391e-16**	**1.1391e-16**	**1.1391e-16**	**1.1391e-16**	**1.1391e-16**	**1.1391e-16**	**1.1391e-16**
	Time/s	0.203490	7.935221	0.198812	0.228899	0.084977	3.740651	29.611148	18.594487	0.113399	0.138919	0.109553	0.314986	0.194977
f_{20}	Best	**-3.322**	-3.0988	**-3.322**	**-3.322**	**-3.322**	**-3.322**	**-3.322**	**-3.322**	**-3.322**	**-3.322**	-3.1505	**-3.322**	**-3.322**
	Mean	-3.2744	-2.7713	-3.2346	-3.2447	**-3.322**	-3.2625	-3.2643	-3.2722	-3.2178	-3.2619	-2.9492	-3.2181	-3.2181
	STD	5.9759e-02	2.1461e-01	5.9011e-02	5.8182e-02	**5.9341e-05**	6.1044e-02	7.4234e-02	6.2692e-02	6.0728e-02	6.1667e-02	2.9042e-01	4.4974e-02	4.4939e-02
	Time/s	0.132421	5.560410	0.159146	0.195733	0.061348	5.271023	16.480948	20.034069	0.090920	0.110095	0.088939	0.154163	0.145909
f_{21}	Best	**-10.1532**	**-10.1532**	**-10.1532**	**-10.1532**	**-10.1532**	**-10.1532**	**-10.1532**	**-10.1532**	**-10.1532**	**-10.1532**	-6.0789	**-10.1532**	**-10.1532**
	Mean	-6.1329	**-10.1531**	-8.1359	-6.7456	-9.8399	-6.3712	-8.3748	-6.6362	-6.5101	-7.4942	-3.0408	-6.3297	-5.3101
	STD	2.8583e+00	**7.2119e-05**	2.8980e+00	2.6226e+00	4.1244e-01	2.9940e+00	2.4850e+00	3.3927e+00	3.1953e+00	2.7795e+00	1.7453e+00	2.2648e+00	1.1399e+00
	Time/s	0.445839	16.394264	0.323969	0.453221	0.227891	3.902405	14.905909	14.024028	0.276735	0.292753	0.263121	0.367920	0.308828
f_{22}	Best	**-10.4029**	**-10.4029**	**-10.4029**	**-10.4029**	**-10.4029**	**-10.4029**	**-10.4029**	**-10.4029**	**-10.4029**	**-10.4029**	-5.5133	**-10.4029**	**-10.4029**
	Mean	-6.0822	**-10.4028**	-9.6385	-8.0556	-9.9179	-6.8891	-9.873	-7.6698	-8.558	-9.1116	-3.271	-6.8312	-5.3534
	STD	3.3159e+00	**9.8426e-05**	2.3528e+00	3.0242e+00	1.0237e+00	3.7150e+00	1.6295e+00	3.2062e+00	2.9360e+00	2.7041e+00	1.6226e+00	2.7378e+00	1.1885e+00
	Time/s	0.889950	30.154814	0.558420	0.784581	0.422006	5.050692	18.679226	19.359965	0.441419	0.483475	0.436974	0.520020	0.505205
f_{23}	Best	**-10.4029**	**-10.4029**	**-10.4029**	**-10.4029**	**-10.4029**	**-10.4029**	**-10.4029**	**-10.4029**	**-10.4029**	**-10.4029**	-9.1017	**-10.4029**	**-10.4029**
	Mean	-6.6255	**-10.4028**	-8.9945	-7.3833	-9.9657	-6.2389	-7.7622	-7.7041	-8.3737	-9.3753	-4.3585	-5.5024	-5.3534
	STD	3.6262e+00	**1.6148e-04**	2.9438e+00	2.8501e+00	5.2114e-01	3.2733e+00	2.7061e+00	3.4847e+00	3.2112e+00	2.5479e+00	1.8357e+00	1.7550e+00	1.1885e+00
	Time/s	0.886499	32.516514	0.555949	0.791533	0.426570	5.051710	16.936576	19.019848	0.457373	0.444934	0.406783	0.564325	0.550653

Appendix C

The description of 15 CEC 2005 benchmark functions is shown in the table below.

Benchmark Functions	Dim	Search Range	f_{min}	Type
F_1: Shifted Sphere Function	5	[-100, 100]	-450	
F_2: Shifted Schwefel's Problem 1.2	5	[-100, 100]	-450	Unimodal
F_3: Shifted Schwefel's Problem 1.2 with Noise in Fitness	5	[-100, 100]	-450	
F_4: Shifted Rotated Ackley's Function with Global Optimum on Bounds	10	[-32, 32]	-140	
F_5: Shifted Rastrigin's Function	10	[-5, 5]	-330	
F_6: Shifted Rotated Rastrigin's Function	10	[-5, 5]	-330	Multimodal
F_7: Shifted Rotated Weierstrass Function	10	[-0.5, 0.5]	90	
F_8: Schwefel's Problem 2.13	10	[-100,100]	-460	
F_9: Shifted Expanded Griewank's plus Rosenbrock's Function (F8F2)	10	[-3, 1]	-130	Multimodal Expanded
F_{10}: Shifted Rotated Expanded Scaffer's F6 Function	10	[-100, 100]	-300	
F_{11}: Rotated Hybrid Composition Function 1 with Noise in Fitness	30	[-5, 5]	120	
F_{12}: Rotated Hybrid Composition Function 2	30	[-5, 5]	10	Multimodal Hybrid Composition
F_{13}: Rotated Hybrid Composition Function 2 with the Global Optimum on the Bounds	30	[-5, 5]	10	
F_{14}: Rotated Hybrid Composition Function 3 with High Condition Number Matrix	30	[-5, 5]	360	
F_{15}: Rotated Hybrid Composition Function 4 without bounds	30	[-2, 5]	260	

Appendix D

The results comparison of the 13 algorithms on 10 CEC 2005 benchmark functions is shown in the table below.

Fun	Index	PSO	AFSA	SSA	SSAPSO	ABC	ALO	DA	GOA	MFO	MVO	SCA	SSA-GWO	DWSSA
	Best	**-450.0000**	-185.6664	**-450.0000**	**-450.0000**	**-450.0000**	**-450.0000**	**-450.0000**	**-450.0000**	**-450.0000**	-449.9993	-435.0813	**-450.0000**	**-450.0000**
F_1	Mean	**-450.0000**	1093.4537	**-450.0000**	**-450.0000**	-449.9881	**-450.0000**	**-450.0000**	**-450.0000**	**-450.0000**	-449.9977	-345.3223	**-450.0000**	**-450.0000**
	STD	3.7896e-14	9.2941e+02	8.5496e-11	6.4431e-11	2.8423e-02	5.1022e-10	1.4767e+01	1.1951e-08	**0**	1.4100e-03	1.0192e+02	6.9431e-11	8.3813e-11
	Best	**-450.0000**	603.7382	**-450.0000**	**-450.0000**	-441.7778	**-450.0000**	-449.9994	**-450.0000**	**-450.0000**	-449.9994	-418.0914	**-450.0000**	**-450.0000**
F_2	Mean	**-450.0000**	2224.0771	**-450.0000**	**-450.0000**	-424.9087	**-450.0000**	-398.6725	-449.9999	-435.8126	-449.9961	-348.5260	**-450.0000**	**-450.0000**
	STD	**7.0896e-14**	1.1735e+03	1.3549e-10	2.4631e-10	2.9211e+01	2.3823e-08	6.7926e+01	1.7524e-04	4.4864e+01	2.6804e-03	4.7641e+01	9.5298e-11	3.4304e-10
	Best	**-450.0000**	803.0037	**-450.0000**	-449.9994	-421.1642	**-450.0000**	-449.7000	**-450.0000**	**-450.0000**	-449.9998	-384.2145	**-450.0000**	**-450.0000**
F_3	Mean	**-450.0000**	4504.8486	**-450.0000**	-445.8334	-143.0147	**-450.0000**	-159.3890	-449.9999	-436.4501	-449.9952	-312.6902	**-450.0000**	**-450.0000**
	STD	**1.8948e-14**	2.4550e+03	8.6664e-10	8.0696e+00	3.0131e+02	1.1672e-06	6.1952e+02	1.8613e-04	4.2849e+01	5.2108e-03	4.8165e+01	3.8470e-10	1.5291e-10
	Best	-119.6728	-119.8007	-119.9060	-119.8502	-119.6226	-119.8419	-119.7464	-119.8634	-119.8103	-119.6726	-119.6370	-119.9271	**-119.9683**
F_4	Mean	-119.5391	-119.6478	-119.7889	-119.4923	-119.4563	-119.7016	-119.5158	-119.6523	-119.6763	-119.4789	-119.4676	-119.7144	**-119.7976**
	STD	8.6600e-02	**6.9901e-02**	7.4468e-02	1.9740e-01	9.2744e-02	1.1362e-01	1.4960e-01	1.1108e-01	1.5673e-01	8.0474e-02	8.6858e-02	1.1270e-01	1.0080e-01
	Best	-307.9472	-254.7834	-318.0605	-318.0605	-326.7743	-304.1311	-297.3407	-307.1158	**-323.0353**	-320.0306	-296.7736	-318.0605	-317.0655
F_5	Mean	-297.6748	-233.7366	-290.3014	-307.2997	**-320.4490**	-290.2914	-281.6543	-269.5832	-307.5602	-302.9018	-283.6922	-299.3773	-290.1102
	STD	9.1911e+00	1.0363e+01	2.0317e+01	7.9383e+00	**3.7401e+00**	1.2555e+01	1.5258e+01	2.7051e+01	1.4544e+01	1.4298e+01	8.6848e+00	1.5450e+01	1.2911e+01
	Best	-299.8374	-220.1063	-311.0958	**-324.0302**	-286.4748	-314.0807	-308.2972	-314.0806	-316.0706	-320.9692	-272.5705	-320.0504	-322.0403
F_6	Mean	-270.9414	-201.0021	-295.0771	**-304.8499**	-265.3277	-298.9127	-273.2878	-278.2978	-296.2464	-308.1670	-263.9704	-298.7584	-299.3116
	STD	2.3117e+01	1.2658e+01	1.8599e+01	1.0875e+01	1.5817e+01	1.1477e+01	3.1708e+01	2.8964e+01	1.4876e+01	8.9113e+00	6.6469e+00	1.1395e+01	1.7853e+01
	Best	97.7820	101.3697	**93.0008**	95.0493	96.5269	0	95.4118	0	95.3372	90.7586	0	94.3743	94.7170
F_7	Mean	99.0808	102.7917	96.1668	98.7066	98.4058	97.0923	97.6008	99.1964	97.6039	94.4477	99.8609	**95.7062**	96.3475
	STD	9.4392e-01	8.9768e-01	1.9874e+00	2.3758e+00	1.1066e+00	1.5727e+00	1.4367e+00	1.8961e+00	1.5025e+00	1.8667e+00	1.1193e+00	**1.0191e+00**	1.1264e+00
	Best	8995.7917	70501.0330	**-455.6090**	-174.8450	634.9145	-407.6530	14399.6493	-395.6209	1734.9514	-99.4921	0	-444.5814	-441.5412
F_8	Mean	37561.7613	133577.9827	1117.2647	51434.9837	3621.0118	516.5828	33099.9678	4479.0146	16032.1551	3175.6611	47424.8078	472.6751	**83.6771**
	STD	1.7389e+04	3.0578e+04	1.5889e+03	3.5262e+04	1.5664e+03	1.7698e+03	1.3768e+04	1.0988e+04	1.1821e+04	2.7255e+03	1.3910e+04	1.1101e+03	**7.2752e+02**
	Best	-129.0411	-122.8923	-129.2638	-129.4235	-129.2649	-129.5395	-128.3999	-129.1323	-129.4485	**-129.3149**	-126.0649	-128.7165	-129.295
F_9	Mean	-127.5767	-119.4241	-127.8385	**-128.7889**	-128.4982	-127.8752	-126.2546	-126.7925	-128.4172	-128.4825	-125.162	-127.8879	-128.3425
	STD	1.1291e+00	2.9632e+00	1.1402e+00	**5.6365e-01**	7.0434e-01	1.4489e+00	2.1935e+00	1.5826e+00	1.0063e+00	8.4001e-01	6.7495e-01	1.2364e+00	6.9044e-01
	Best	-296.9412	-295.4999	-297.8358	-296.5167	-296.9807	-296.7956	-296.2134	-296.9608	-296.4278	**-297.1257**	-296.6516	-296.8790	-296.7859
F_{10}	Mean	-296.3176	-295.4218	-296.3214	-296.1942	-296.0431	-296.1130	-295.8860	-296.2415	-296.0743	**-296.5553**	-296.0788	-296.1963	-296.2717
	STD	3.2655e-01	5.3238e-02	5.7883e-01	2.2937e-01	3.9188e-01	3.3846e-01	**2.1296e-01**	4.1893e-01	2.5834e-01	3.7860e-01	2.8175e-01	2.9210e-01	2.7493e-01
	Best	409.0809	1296.0074	**130.5527**	579.5881	511.2674	0	583.1904	0	151.6622	18.6598	0	101.64	162.795
F_{11}	Mean	614.9906	1392.1815	300.7147	2083.2697	603.3323	505.4262	761.8350	473.7460	233.2034	**129.6592**	532.8881	275.8389	229.6506
	STD	8.7017e+01	8.5069e+01	1.3653e+02	3.7042e+02	1.0764e+02	2.0681e+02	1.3461e+02	1.2355e+02	9.3758e+02	1.7796e+02	2.9674e+02	1.1409e+02	**8.0958e+01**
	Best	135.8234	10	26.7526	11.5502	101.0539	0	97.1926	0	21.0329	16.7648	0	**10**	**10**
F_{12}	Mean	184.1505	10.0001	34.1131	62.6713	183.7798	157.0065	215.9682	121.7593	45.6927	22.0521	237.253	**10**	**10**
	STD	4.5776e+01	9.4421e-05	6.0264e+00	3.5401e+01	9.9557e+01	3.7054e+01	8.5622e+01	6.4854e+01	2.2105e+01	3.3363e+00	3.5920e+01	**0**	**0**
	Best	223.3900	10	23.4916	14.4068	97.3166	0	138.0306	0	26.3676	19.0650	0	**10**	**10**
F_{13}	Mean	282.9021	10.0001	36.8976	56.4174	141.7528	170.3248	246.6336	134.8865	54.4895	22.0383	230.3960	**10**	**10**
	STD	5.7958e+01	8.9427e-05	1.2673e+01	2.7829e+01	3.6500e+01	6.4277e+01	1.0764e+02	8.1017e+01	2.6648e+01	2.5390e+00	3.5829e+01	**0**	**0**
	Best	913.0658	1821.8177	677.7068	**560.8716**	771.6942	0	873.3534	0	570.7918	670.4211	0	590.2953	608.9984
F_{14}	Mean	1036.606	1889.2734	729.9071	**644.3113**	909.4561	787.7768	976.2354	758.8764	657.5231	791.3149	897.7997	646.5544	674.0601
	STD	1.1052e+02	7.6086e+01	4.8672e+01	6.0754e+01	1.1746e+02	3.0154e+01	7.7335e+01	1.6077e+02	9.7501e+01	7.36901e+01	5.5251e+01	5.0586e+01	**4.1567e+01**
	Best	1373.8376	1490.2524	1089.4471	**431.9926**	1400.6348	0	1391.6508	0	1088.1291	1021.9371	0	1088.986	1242.271
F_{15}	Mean	1420.2859	1493.6074	1271.1332	**677.6187**	1440.1504	1354.8655	1416.3205	1380.8715	1157.013	1129.5048	1347.8076	1200.1161	1293.2887
	STD	1.5964e+01	**2.7710e+00**	1.1249e+02	198.3728	2.4149e+01	1.0129e+01	2.0949e+01	6.7029e+01	9.5046e+01	1.1857e+02	7.6064e+00	7.7410e+01	5.0005e+01

References

Ashouri-Zadeh, A. , Toulabi, M. , Dobakhshari, A. S. , Taghipour-Broujeni, S. , Ranjbar, A. M., 2018. A novel technique to extract the maximum power of photovoltaic array in partial shading conditions. Inter. J. Ele. Power 101, 500-512.

Abdalla, I., Corda, J., Zhang, L., 2016. Optimal control of a multilevel dc-link converter photovoltaic system for maximum power generation. Renew. Energy 92, 1-11.

Ayop, R., Tan, C.W., 2018. Design of boost converter based on maximum power point resistance for photovoltaic applications. Sol. Energy 160, 322-335.

Ali, I.R., Ewees, A.A., Diego, O., Mohamed, A.E., Li S.F., 2018. Improved salp swarm algorithm based on particle swarm optimization for feature selection. J. Amb. Intel. Hum. Comp.

Batarseh, M.G., Za"Ter, M.E., 2018. Hybrid maximum power point tracking techniques: a comparative survey, suggested classification and uninvestigated combinations. Sol. Energy 169, 535-555.

Bruckner, T., Bemet, S., 2001. Loss balancing in three-level voltage source inverters applying active NPC switches. In 2001 IEEE 32nd Annual Power Electronics Specialists Conference, 2, 1135-1140.

Bishop, J.W., 1988. Computer simulation of the effects of electrical mismatches in photovoltaic cell interconnection circuits. Sol. C. 25(1), 73-89.

Chen, C.W. , Chen, K.H., Chen, Y.M., 2014. Modeling and controller design of an autonomous pv module for dmppt pv systems. IEEE Trans. Power Electron. 29(9), 4723-4732.

Chiang, S.J., Shieh, H.J., Chen, M.C., 2009. Modeling and control of pv charger system with sepic converter. IEEE Trans. Ind. Electron. 56(11), 4344-4353.

Floricau, D., Floricau, E., Dumitrescu, M., 2008. Natural doubling of the apparent switching frequency using three-level ANPC converter. IEEE International School on Nonsinusoidal Currents and Compensation.

Jiang, L.L., Srivatsan, R., Maskell, D.L., 2018. Computational intelligence techniques for maximum power point tracking in PV systems: A review. Renew. Sustain. Energy Rev. 85, 14-45.

Kumar, R., Singh, B., 2016. BLDC motor-driven solar PV array-fed water pumping system employing zeta converter. IEEE Trans. Ind. Appl. 52(3), 2315-2322.

Khan, M.J., Mathew, L., 2018. Fuzzy logic controller-based MPPT for hybrid photo-voltaic/wind/fuel cell power system. Neural Computing and Applications, 1-14.

Kennedy J., Eberhart R., 1995. Particle swarm optimization[C]// Proceedings of ICNN'95 - International Conference on Neural Networks.

Karaboga, D., Basturk, B., 2007. A powerful and efficient algorithm for numerical function optimization: artificial bee colony (ABC) algorithm. J.Global Optim. 39(3), 459-471.

Khalil H K, 2015. Lyapunov's Stability Theory[M]. Springer London.

Li, H., Yang, D., Su, W., Lu, J., Yu, X., 2018. An overall distribution particle swarm optimization mppt algorithm for photovoltaic system under partial shading. IEEE Trans. Ind. Electron. 99, 1-1.

Luo, H., Wen, H., Li, X., Jiang, L., Hu, Y., 2016. Synchronous buck converter based low-cost and high-efficiency sub-module DMPPT PV system under partial shading conditions. Energ.Convers.Manage. 126, 473-487.

Li, X.L., 2002. An optimizing method based on autonomous animats: fish-swarm algorithm. Syst. Eng.Theo. Prac. 22(11), 32-38.

Martin, A. D., Vazquez, J. R., Cano, J. M., 2018. MPPT in PV systems under partial shading conditions using artificial vision. Elec. Pow. Syst. Res. 162, 89-98.

Messalti, S., Harrag, A., Loukriz, A., 2017. A new variable step size neural networks mppt controller: review, simulation and hardware implementation. Renew. Sustain. Energy Rev. 68, 221-233.

Mao, M., Duan, Q., Yang, Z., Duan, P., 2016. Modeling and global MPPT for PV system under partial shading conditions using modified artificial fish swarm algorithm. IEEE International Symposium on

Systems Engineering.

Mao, M., Zhang, L., Duan, P., Duan, Q., Yang, M., 2018. Grid-connected modular PV-Converter system with shuffled frog leaping algorithm based DMPPT controller. Energy 143, 181-190.

Mohanty, S., Subudhi, B., Ray, P.K., 2015. A new MPPT design using grey wolf optimization technique for photovoltaic system under partial shading conditions. IEEE Trans. Sustain. Energy 7(1), 181-188.

Mirjalili, S., 2015. The ant lion optimizer. Adv. Eng. Softw. 83, 80-98.

Mirjalili, S., 2016. Dragonfly algorithm: a new meta-heuristic optimization technique for solving single-objective, discrete, and multi-objective problems. Neur. Comp. Appl. 27(4), 1053-1073.

Mirjalili, S., 2015. Moth-flame optimization algorithm: A novel nature-inspired heuristic paradigm. Knowl.-Based Syst. 89, 228-249.

Mirjalili, S., Mirjalili, S.M.,Hatamlou, A., 2016. Multi-verse optimizer: a nature-inspired algorithm for global optimization. Neur. Comp. Appl. 27(2), 495-513.

Mirjalili, S., 2016. SCA: a sine cosine algorithm for solving optimization problems. Knowl.-Based Syst. 96, 120-133.

Naderi, R., Wu, B., Smedley, K., 2016. Analysis of a distributed maximum power point tracking tracker with low input voltage ripple and flexible gain range. IET Power Electron. 9(6):1220-1227.

Prabaharan, N., Palanisamy, K., 2016. Analysis and integration of multilevel inverter configuration with boost converters in a photovoltaic system. Energ.Convers.Manage. 128, 327-342.

Peng, L., Zheng, S., Chai, X., Li, L., 2018. A novel tangent error maximum power point tracking algorithm for photovoltaic system under fast multi-changing solar irradiances. Appl. Energy 210, 303-316.

Rizzo, S. A., Salerno, N., Scelba, G., Sciacca, A.,2018. Enhanced hybrid global mppt algorithm for pv systems operating under fast-changing partial shading conditions. Inter. J. Renew. Energy Res. 8(1).

Soufyane Benyoucef, A., Chouder, A., Kara, K., Silvestre, S., 2015. Artificial bee colony based algorithm for maximum power point tracking (MPPT) for PV systems operating under partial shaded conditions. Appl. S. Comput. 32, 38-48.

Shahid, H., Kamran, M., Mehmood, Z., Saleem, M.Y., Mudassar, M., Haider, K., 2018. Implementation of the novel temperature controller and incremental conductance mppt algorithm for indoor photovoltaic system. Sol. Energy 163, 235-242.

Seyedali M., Amir H.G., Seyedeh Z.M., 2017. Salp Swarm Algorithm: A Bio-inspired Optimizer for Engineering Design Problems. Adv. Eng. Softw.114(1), 163-191.

Saremi, S., Mirjalili, S., Lewis, A., 2017. Grasshopper optimisation algorithm: theory and application. Adv. Eng. Softw. 105, 30-47.

Teshome, D., Lee, C.H., Lin, Y.W., Lian, K.L., 2016. A modified firefly algorithm for photovoltaic maximum power point tracking control under partial shading. IEEE J. Em. Sel. Top. Power Electron. 1-1.

Tey, K.S., Mekhilef, S., Seyedmahmoudian, M., Horan, B., Stojcevski, A., 2018. Improved differential evolution-based mppt algorithm using sepic for pv systems under partial shading conditions and load variation. IEEE Trans. Ind. Electron. 99, 1-1.

Urtasun, A., Lu, D.C., 2015. Control of a single-switch two-input buck converter for mppt of two pv strings. IEEE Trans. Ind. Electron. 62(11), 7051-7060.

Urtasun, A., Sanchis, P., Marroyo, L., 2013. Adaptive voltage control of the dc/dc boost stage in pv converters with small input capacitor. IEEE Trans. Power Electron. 28(11), 5038-5048.

VillalvaM.G., GazoliJ.R., FilhoE.R., 2009. Comprehensive approach to modeling and simulation of photovoltaic arrays. IEEE Trans. Power Electron. 24 (5), 1198–1208.

Walker, G.R., Sernia, P.C., 2004. Cascaded dc-dc converter connection of photovoltaic modules. IEEE Trans. Power Electron. 19(4), 1130-1139.

Wan Y., Mao M., Zhou L., 2019. A Novel Nature-Inspired Maximum Power Point Tracking (MPPT) Controller Based on SSA-GWO Algorithm for Partially Shaded Photovoltaic Systems. Electron. 8(6), 680.